



Review

Sulfonated mesoporous carbon and silica-carbon nanocomposites for biomass conversion

Ruyi Zhong^{a,b,*}, Bert F. Sels^{c,***}^a Department of Chemistry, Southern University of Science and Technology, Xueyuan Road 1088, 518055, Shenzhen, China^b Dalian Institute of Chemical Physics, Chinese Academy of Sciences, Zhongshan Road 457, 116023, Dalian, China^c Centre for Surface Science and Catalysis, KU Leuven, Corelab, Celestijnlaan 200F, B3001, Heverlee, Belgium

ARTICLE INFO

Keywords:

Sulfonated mesoporous silica-carbon nanocomposites
Evaporation induced triconstituent co-assembly
Carbonization
Sulfonation
Biomass conversion

ABSTRACT

Sulfonated mesoporous carbon or silica-carbon nanocomposite materials possess a large amount of accessible SO_3H acid groups, which may have versatile applications as solid acid catalysts in biomass conversion. The mesopores can facilitate the transportation of the large biomass substrates and the targeted products. The hydrophobicity of carbon ensures the hydrothermal stability of the materials, which is essential since biomass conversion usually occurs in polar circumstances (e.g., in water), and it can facilitate the adsorption of reactants and the desorption of formed H_2O during the conversion simultaneously. The other weak acid groups of carbon, like phenolic OH and COOH groups may help the adsorption of reactants or even exert a synergistic catalytic function. With the co-existence of silica phase, the mesopores can be maintained under harsh conditions, e.g., during the sulfonation synthesis step in concentrated H_2SO_4 at a high temperature. Furthermore, the hybrid silica-carbon surface can provide specific polarity from the synergy of both kinds of components and offer potentiality for multi-functionalization. Herein, the synthesis and fabrication of such sulfonated mesoporous carbon and silica-carbon nanocomposite wherein $\text{C}-\text{SO}_3\text{H}$ is confined in mesoporous channels is reviewed. Their state-of-the-art use in catalytic biomass-related conversion such as fatty acids esterification, carbohydrates conversion and furan-derivative condensation, are discussed in detail. The stability issues of the sulfonated carbon or silica-carbon nanocomposites for the specific catalytic reactions are specifically addressed. Finally, a general conclusion is drawn from the above and a future outlook for this class of upcoming materials in terms of synthetic challenges and catalytic application is presented.

1. Ordered mesoporous structure (OMS)

Since the first discovery of mesoporous silica, hexagonally ordered MCM-41 in 1992 by Mobil group, well-ordered mesoporous materials characterized by a precise periodic arrangement of mono-sized pores have stimulated intensive research interests [1–3]. They exhibit large uniform mesopores (from 2 to 50 nm in pore diameter), surface areas and pore volumes that underline their significant applications in various fields, such as catalysis [2,4–11] adsorption [12,13], energy storage [14,15], drug delivery [16,17], sensors [18,19], etc. Besides the mesoporous silica family which mainly includes M41S family [2] and SBA series [3], there have been considerable efforts to incorporate an organic component for an “active” pore surface for easy modification or functionalization, i.e., organic-inorganic hybrid framework [5,16,20–25], or fabricate ordered mesoporous polymers and carbons [7,14,26–31]. These mesoporous silica-carbon nanocomposites -

nanohybrids will be used when the two different building blocks are covalently bonded [20] - and mesoporous carbons hold many attractive features, such as the surface hydrophobicity, high corrosion resistance, as well as good thermal and mechanical stability [21–24,32], in addition to the mesoporous structures. Ordered mesoporous carbon or silica-carbon nanocomposite can be intentionally synthesized with the assistance of structure-directing agents (SDA) or templates, either by the hard-template method using porous solid-state templates as sacrificial or supporting scaffolds or by the soft-template method employing amphiphilic block copolymers as structure-directing agents.

1.1. Hard templating

Hard-templating method is also known as “nano-casting” [28,33–36], which includes the infiltration of nanochannels of a rigid inorganic solid with an appropriate carbon precursor, followed by

* Corresponding author.

** Corresponding author.

E-mail addresses: zhongrui@sustc.edu.cn, zhongrui@dicp.ac.cn (R. Zhong), bert.sels@kuleuven.be (B.F. Sels).

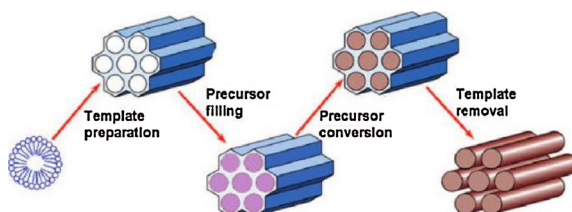


Fig. 1. Schematic illustration for the nanocasting strategy. Reproduced with permission from Ref. [26]. Copyright 2008 American Chemical Society.

further carbonization into the desired materials, as schematically illustrated in Fig. 1. The removal (or not) of the hard-template depends on the porosity of the resultant carbon, whose framework should be not be collapsed after the removal of template, and upon applying of the material [37]. The pores can be partly filled (coated) with carbon to form hard-templated silica-carbon nanocomposites, which gives high catalytic performance for esterification of oleic acid [38,39], ethanalysis of 5-hydroxymethylfurfural (HMF) [40], dimerization of α -methylstyrene [41], etc. They also showed a high separation factor with high sorption capacities in the separation of linear from branched alkanes [42]. Compared to carbonaceous materials, silica-carbon nanocomposites possess improved thermal and mechanical stability [43,44], and a higher proportion of stronger acid sites can be created after sulfonation [41,45].

Ordered mesoporous carbon was firstly synthesized by Ryoo's group [33] and Hyeon's group [36] in 1999 by condensing sucrose into carbon under the catalysis of H_2SO_4 inside the mesopores of MCM-48 (CMK-1) and by converting phenol-formaldehyde inside the mesopores of Al-MCM-48 (SNU-1) respectively. After removal by acid [36] or base [33] etching process, ordered mesoporous carbon was retrieved from the silica-carbon composite. Various carbon precursors besides sucrose and phenolic resin have been applied today in the hard template synthesis, such as glucose [41,46], glycerol [47], furfuryl alcohol [42,48,49], 2,3-dihydroxynaphthalene [38,50], *p*-toluenesulfonic acid [40], thiophene [51], pyrrole [51], aniline [52], ionic liquids [53], chloromethylstyrene [54], etc. Most of the carbon precursors can be condensed into carbon phase upon thermal treatment, but in order to avoid random incorporation, initiator such as azoisobutyronitrile (AIBN) [54,55] was also applied to realize a controllable polymerization inside the porous hard template. The hard-templates include MCM-41 [35,42,48], SBA-15 [38–41,46,47,49–55], KIT-6 [38,51], mesocellular silica [38,40], etc. The surface of the hard templates can also be functionalized to serve simultaneously as a catalyst for the carbonization of carbon precursors. For example, SBA-15 was coated with Fe [56] or MCM-41 was treated with $AlCl_3$ [35] to promote the carbonization of phenolic resins, while mesoporous silica-initiator nanospheres [57] were fabricated to realize surface confined atom transfer radical polymerization (ATRP) of methacrylate monomers.

The hard template method corresponds to the grafting strategy (post synthesis) in the synthesis of organosilica (silica-carbon nanohybrid) [5,8,22,25], in contrast to the one-pot co-condensation through self-assembling micellar routes (direct synthesis). The mesoporous silica surface is modified with organic groups through silylation reactions occurring on silanol groups using trichloro-, trialkoxyorganosilane or silylamines as the organic precursors [5]. For example, vinyl-grafted MCM-41 sample was obtained by refluxing MCM-41 in a vinyl-trichlorosilane-containing toluene solution [58].

Although the hard template method has been widely applied and successfully retained or replicated the mesoporous structure, this method has the significant drawback that scale-up for industrial applications is highly difficult, due to the complicated and time-consuming synthesis and the comparatively high cost of using the pre-formed mesoporous silica as a scaffold. Besides, as an exo-template method is used, the template needs to be wetted by the precursor

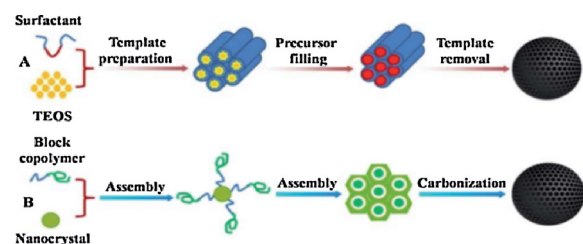


Fig. 2. Schematic illustrations of (A) a hard-template method and (B) a soft-template method for the synthesis of ordered mesoporous carbon. Reproduced with permission from Ref. [31]. Copyright 2015 Royal Society of Chemistry.

molecules, and thus suffers from a random distribution of the carbon constituent, pore blockage, phase separation and a disordered pore architecture [20,27]. Some relatively cheap hard templates, like silica gel (K100) [59], fumed SiO_2 [45] and alumina membrane [60] were applied instead of ordered mesoporous silica, and then only micro-porosity and/or macroporosity were obtained.

1.2. Soft templating

The soft template method which employs self-assembled structures composed of soft organic materials, has emerged as an alternative to overcome the limitations of the hard template method. As shown in Fig. 2, the key point of the soft-templating route lies in endo-templating, that is the direct use of the self-assembly of the surfactant polymer as the structure-directing agent (SDA), which makes the synthesis simpler and more scalable. Typical soft templates include block copolymers like poly(ethylene oxide)-block-poly(propylene oxide)-block-poly(ethylene oxide) (Pluronic F127 PEO_{106} - PPO_{70} - PEO_{106} and Pluronic P123 PEO_{20} - PPO_{70} - PEO_{20}) [61,62] and polystyrene-block-poly(4-vinylpyridine) (PS-P4VP) [63]. The structure-directing agent in the soft-template synthesis of mesostructured silica materials can be employed as a carbon source at the same time, with the aid of H_2SO_4 [64,65] or using the thermosetting nature of the surfactant ($PEO-b-PS$) [66]. The mostly adopted carbon precursor for the soft-template synthesis for mesoporous carbon or silica-carbon nanocomposite is phenolic resins and their derivatives [27,31,67]. Later, the application of sucrose as a non-toxic and economical carbon substituent was suggested [68].

There are two main pathways in the soft template synthesis of ordered mesoporous material, namely, cooperative self-assembly (CSA) and liquid-crystal templating (LCT), as shown in Fig. 3 [72]. In the CSA mechanism, the cooperative organization of the already added precursor species and the surfactants molecules occurs to form a mesostructured lyotropic liquid-crystalline phase. The liquid-crystal phase can be developed at lower concentrations of surfactant according to the CSA mechanism. This mechanism was later proven by *in situ* Small Angle X-ray or Neutron Scattering (SAXS or SANS) in the sol-gel synthesis of mesoporous silica materials, as the hybrid silica-surfactant micellar aggregates prior to the precipitation of the material were detected [70]. In the LCT mechanism, the surfactant molecules organize into true or semi-liquid crystal mesophase micelles after reaching the critical micelle concentration (CMC) and the formed lyotropic liquid crystalline phase serves as a template for the incorporation of precursors for the formation of the mesostructure. The versatile evaporation induced self-assembly (EISA) can be assigned to this mechanism, as the highly concentrated surfactants form liquid-crystal phases in the presence of precursors during the final stage of solvent evaporation [69,71].

For the soft template synthesis of ordered mesoporous silica, there are many self-assembly driving forces under different pH conditions [2], such as I^-S^+ , $I^+X^-S^-$, I^+S^- , where I is inorganic precursor, S is surfactant and X^- is the anion. However, for the direct organization of surfactant and organic precursor, mainly self-assembly induced by

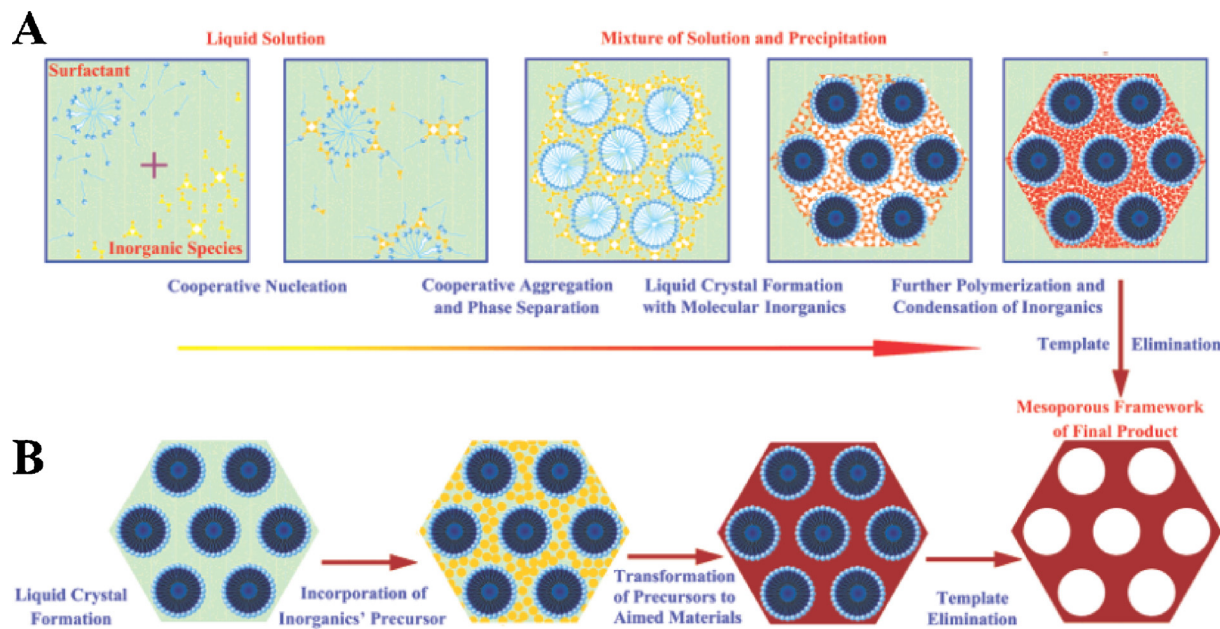


Fig. 3. Formation of mesoporous structures: (A) via co-operative self-assembly (CSA), (B) via true liquid-crystal templating (LCT) process. Reproduced with permission from Ref. [72]. Copyright 2013 Royal Society of Chemistry.

hydrogen-bonding ($\text{I}^{\circ}\text{S}^{\circ}$) has been utilized [26,27,67]. Only under highly acidic conditions where the protonation of precursor molecules and the EO blocks of Pluronic F127 were induced, Coulombic interactions using Cl^- as a mediator can facilitate the self-assembly *via* the $\text{I}^+\text{X}^-\text{S}^+$ mechanism [73,74]. The introduction of the inorganic silica precursor to the organic polymeric network, *i.e.*, making a mesoporous silica-carbon nanocomposite, can assist in the organization into ordered mesostructures by constructing a “reinforced-concrete” framework, since abundant $\text{Si}-\text{OH}$ groups can provide strong interaction with the surfactant [43,44].

The soft-template method corresponds to the co-condensation strategy in the organosilica nanohybrid synthesis. There are many successful examples of constructing periodic mesoporous organosilica matrix with various bridged silsequioxanes in the pore wall by co-condensation [5,8,25]. The vinyl-MCM-41 produced from the one-pot direct synthesis of vinyltrichlorosilane and tetraethoxysilane (TEOS) in the presence of cetyltrimethylammonium bromide (CTAB) contains uniformly distributed vinyl groups at the walls, compared to the counterpart from the post-synthetic grafting [58]. However, it should be noticed that the use of functionalized organosiloxane precursor is quite expensive and due to its hydrophobic characteristic, the assembly with template micelles becomes more complicated and difficult [22,25].

1.2.1. Evaporation-induced self-assembly (EISA)

The predominant approach applied for organic-organic self-assembly is the EISA method [26,34,75]. EISA method consists in casting films of the synthesis solution by coating a planar surface during spin-coating [63,76,77], dip-coating [78–80], petri-dish-coating [61,81], etc. This method was firstly applied to the preparation of continuous mesoporous silica films [78,79]. The precursor silica oligomers and surfactant form a homogeneous solution in a solvent with weak polarity (for example in ethanol). With the preferential evaporation of ethanol, the surfactant concentration progressively increases and drives the self-assembly of silica-surfactant micelles and their further organization into liquid-crystalline mesophases [71,78,79]. The final mesostructure is affected by the hydrolysis and cross-linkage of inorganic precursors, the nature of surfactants, and the ratio of surfactant/inorganic precursors, similar to the sol-gel aqueous process [69,71,82]. Moreover, as EISA utilizes a concentration gradient starting from the liquid-gas

interface to induce the ordering of precursors around templates [30,71], many other factors like processing humidity [83], evaporating temperature and rate [84], liquid film thickness [71,84], etc. In thick cast films, multi-phases (disordered regions) are more likely to be formed [84–86], due to the slowed evaporation of solvent, the increased condensation degree of precursor species and viscosity, the decreased mobility of entities, etc. [83,84,87].

Despite its limitations for fabricating bulk-materials, EISA has been proven to be a powerful route for preparing ordered mesoporous carbon or silica-carbon nanocomposites. Ordered mesostructure containing resorcinol-formaldehyde/triethyl orthoacetate (carbon precursors) and F127 (template) was constructed [76], and the addition of triethyl orthoacetate helped to reduce the condensation rate of resorcinol-formaldehyde to avoid amorphous phase [26]. Zhao and co-workers prepared different mesoporous carbon structures (2D hexagonal, 3D bicontinuous, body-centered cubic and lamellar, as shown in Fig. 4) by simply adjusting the ratio of phenolic resol (low-polymerized phenol-formaldehyde) to Pluronic surfactant template [61,81]. A study using the spin probe electron paramagnetic resonance (EPR) found that the relatively hydrophilic resol forms a composite with the PEO-PPO-PEO micelles through hydrogen bonding with the PEO block during the evaporation of ethanol [88]. The resol penetrates all the way to the PPO-PEO interface which gets better segregated and forms the fixed mesostructure in the next thermopolymerization step [88]. Zhao's group also achieved a 2D hexagonally mesoporous silica-carbon nanocomposite from phenolic resol/TEOS/F127 [43] or furfuryl alcohol/3-(triethoxysilyl)furan/TEOS/F127 [44] in ethanol/ $\text{H}_2\text{O}/\text{HCl}$ mixed solution through EISA. They added silica precursor and carbon precursor in sequence to the ethanolic solution of F127. Silica oligomers and resol both have plenty of $-\text{OH}$ groups for the hydrogen-bonding with the hydrophilic PEO blocks of the amphiphilic F127 micelles for the constructing of mesostructure with different polymer/ SiO_2 mass ratios from zero to infinity (Fig. 5) [43]. The final composite consists of interpenetrated framework with “reinforcing-steel-bar” silicate and “concrete” resin are only weakly bonded through $\text{Si}-\text{O}-\text{C}$ (weaker than $\text{Si}-\text{O}-\text{Si}$ and $\text{C}-\text{C}$ bonds individually formed in the silica and carbon phase) [43]. Resol/TEOS/F127 has been proven to be able to co-assemble into ordered mesostructure (34–82 wt% of SiO_2 in the composite after pyrolysis in N_2 at 600 °C) *via* a prolonged EISA process [89], which allows the liquid film

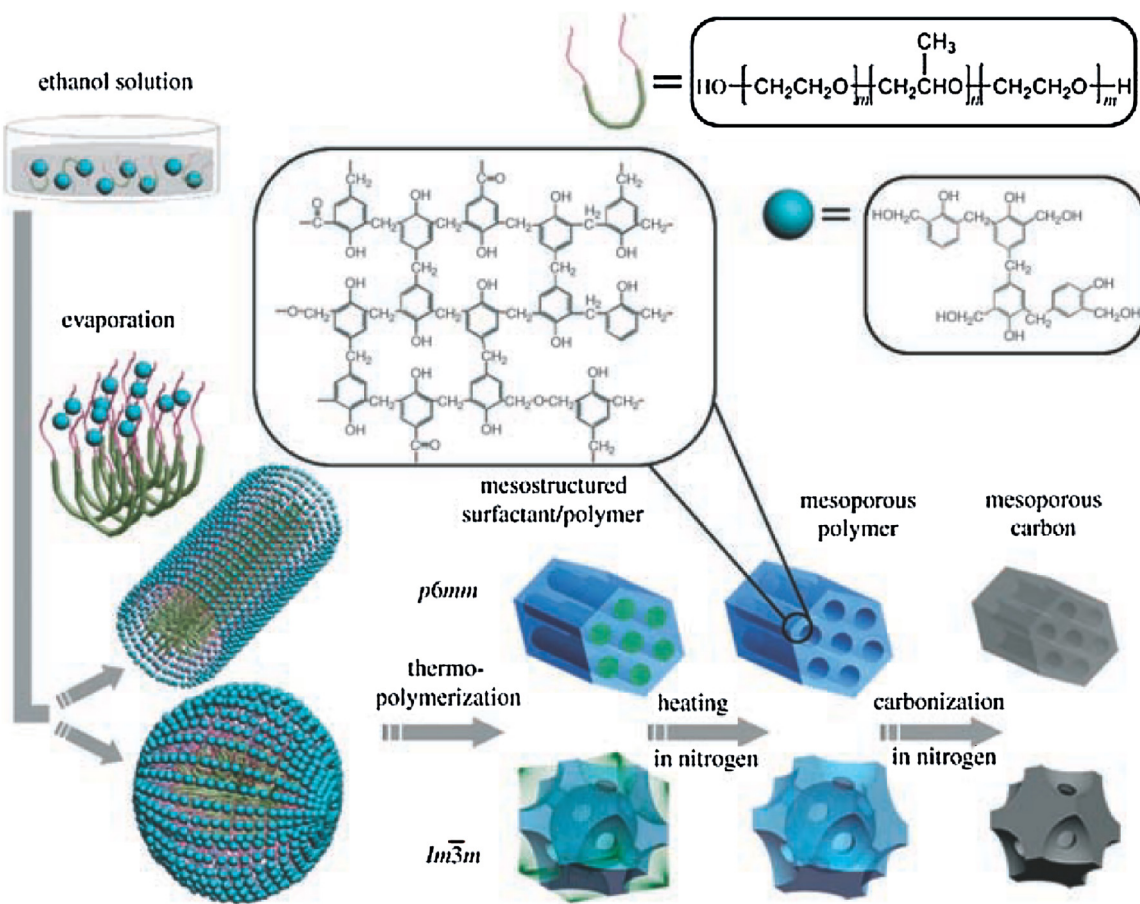


Fig. 4. Scheme for preparation of ordered mesoporous polymer resins and carbon frameworks via EISA. Reproduced with permission from Ref. [61]. Copyright 2005 Wiley.

thickness to be as thick as 3 mm [89], and the operation through large-scale roll-to-roll fabrication using a starting solution film of 0.4 mm thickness [90]. In contrast, due to the linear and hydrophobic poly(furfuryl alcohol), it has to form mesostructure with F127 in the assistance of silicates and the mesostructure collapses after removal of the silicate [44]. Besides, organosilane 3-(triethoxysilyl)furan needs to be introduced to link the poly(furfuryl alcohol) and silicates with covalent C–C and Si–O–Si bonds for the formation of ordered mesostructure [44].

It can also be carried out with an aerosol method (or spray-coating) to realize the fast evaporation of solvent and mesoporous powdery samples were obtained [71,77,78,91]. Fan and co-workers reported the synthesis of mesostructured carbon particles through self-assembly of PS-P4VP and sucrose in the aerosol processing with the evaporation of dimethyl formamide [77]. Lu and co-workers employed the aerosol process to realize the multi-component assembly of resol/TEOS/F127 for an ordered mesostructure with the evaporation of ethanol [91].

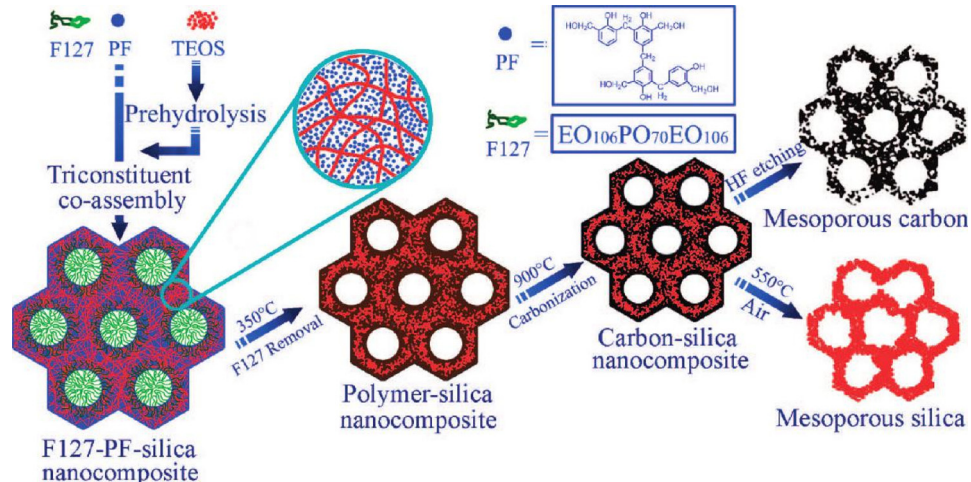


Fig. 5. Triconstituent co-assembly to ordered mesoporous silica-polymer and silica-carbon nanocomposites, as well the corresponding ordered mesoporous silica and carbon frameworks. Reproduced with permission from Ref. [43]. Copyright 2006 American Chemical Society.

1.2.2. Evaporation-induced aggregation assembly (EIAA)

When the block copolymers with long rigid hydrophobic segments, such as PEO-*b*-PS, are applied to the synthesis, according to self-organized precipitation of such block copolymer, the self-assembly of forming the mesostructured precursor-template composite can be performed at the liquid-liquid interface [66,82,92]. Zhao and co-workers used PEO-*b*-PS as a template, TEOS as a silica precursor and resol as a carbon precursor in the acidic THF/H₂O mixture to make a 3D ordered mesoporous silica-carbon nanocomposite [92]. Since H₂O is a poor solvent for PS segments but good for PEO ones, with the evaporation of THF, spherical micelles are formed with PS as a core surrounded by a PEO shell, which is associated with silicate and resol through hydrogen bonding. The increasing composite micelles at the THF-H₂O interface precipitate and pack into an ordered fcc mesostructure as a result of minimizing the interface energy. This synthesis system is less sensitive to H₂O compared to EISA method.

1.2.3. Macroscopic phase separation

When resorcinol/formaldehyde or phloroglucinol/formaldehyde is used as carbon precursor with Pluronic block copolymer under highly acidic conditions in the mixed solution of EtOH and H₂O, macroscopic phase separation to a polymer rich gel phase and a liquid solvent occurs [62,73,85,93,94]. The presence of a high concentration of HCl can control the polymerization rate and provide resorcinol or phloroglucinol with protons to interact with F127 template (I⁺X⁻S⁺ mechanism), along with the hydrogen-bonding interaction (I⁺S⁺) [62,73]. When the polymerization degree of the oligomers is relatively large, the composite of oligomers and F127 will separate from the solvent and form the polymer gel phase, which is separated, cured and carbonized to form the mesoporous carbon [27,93]. Jaroniec and co-workers introduced TEOS or tri(3-trimethoxysilylpropyl)isocyanurate to the resorcinol/formaldehyde carbon precursor to co-assemble with F127 in highly acidic EtOH-H₂O solution [95]. After discarding the aqueous phase, the polymeric layer was dried and carbonized to give an ordered mesoporous silica-carbon composite structure where very small silica domains were uniformly embedded [95]. Though the macroscopic phase separation approach is convenient for the synthesis of large quantities of powdery samples, it shows less ordered structure compared to the counterpart from EISA synthesis [86]. An elongation of aging time helps to reduce defects in the structure [27].

1.2.4. Hydrothermal autoclaving process

A hydrothermal autoclaving process was developed for the synthesis of mesoporous carbon particles [96,97] or monoliths [98–100]. Yuan and co-workers employed resorcinol/formaldehyde precursor with F127 template in a mixed EtOH-H₂O acidic solution under a mild autoclaving treatment at 50 °C for 2 days. They proposed the temperature and autogenous pressure enhance the interactions between molecules and induce the faster polymerization, which lead to the periodic assembly during the mild macroscopic phase separation [99]. Zhao and co-workers used resol and F127 in basic [96] or strong acidic H₂O solution [97] via a hydrothermal autoclaving treatment at 130 °C for 24 h [96] or 120 °C for 12 h [97] and obtained mesoporous carbon nanospheres. Xiao and co-workers performed the autoclaving treatment at 100–260 °C for 17 h with resol/F127 in basic solution. They found that the high temperature (200–260 °C) decomposed a large amount of F127 and increased the cross-linking degree of resin but did not influence the well-ordered mesostructure [101]. Qi et al. [102] and Lei et al. [103] employed hexamethyltetramine as an alternative cross-linker of formaldehyde, and they prepared mesoporous carbon material from resol/F127 [102] and resorcinol/F127 [103] under autoclaving processing respectively. Biomass-derived materials, such as fructose[100] and β-cyclodextrin [98] were also applied as carbon precursor to assemble with F127 in H₂O at 130 °C for 3–5 days [100] or in acidic H₂O at 140 °C for 36 h [98]. The HMF from hexose dehydration was presumed to be polymerized and interact with the PEO segments of F127 through

hydrogen-bonding to form the ordered mesostructure [98,100]. This hydrothermal autoclaving method requires relatively long synthesis time and high energy consumption for the temperature and pressure.

1.2.5. Dilute aqueous route

Zhao and co-workers reported the synthesis of ordered mesoporous carbon by a dilute aqueous route using Pluronic triblock copolymer as template and resol as carbon precursor [104,105]. This method requires a narrow pH range during the synthesis (pH = 8.5–9), since the hydrogen-bonding with the template is weakened at pH above 9, while the polymerization is too slow at pH below 8.5 [27,28,104,105]. The mechanism of the self-assembly in the dilute solution is supposed to follow the CSA route, that is, the resol forms complexes with the copolymer through hydrogen-bonding with the PEO blocks and the resulting complexes further assemble into the mesostructure, similar to the formation of mesostructured silicates from surfactant induced self-assembly in aqueous solution [104,105]. As an improvement to the aqueous synthesis, Lei and co-workers replaced formaldehyde with hexamine as a release source of formaldehyde, which can control the polymerization rate of resorcinol and the self-assembly [106].

1.2.6. Solution-phase synthesis for silica-carbon nanocomposite

Solution phase synthesis for silica-carbon nanocomposite is challenging, due to the different polymerization rates of inorganic and organic species that can destroy the co-assembly and leads to the disordered arrangement [43,44]. Hyeon and co-workers added phenol, silica source and formaldehyde in sequence to H₂O solution containing P123 and HCl to form the phenolic resin/silica/P123 composite, but they obtained wormhole-like mesopores after the removal of P123 [107]. Song's group and Kao's group utilized carbon source such as sucrose [108–110], glycerol [111], and butanol [112] as a co-template, which was assembled with P123 prior to being a structure-directing agent for silica oligomers. The as-synthesized carbon precursor/silica/P123 composite was carbonized in the assistance of H₂SO₄, which acted as a catalyst for the cross-linking of P123 and sucrose [108–110]. The resultant silica-carbon nanocomposite was used as precursor for mesoporous carbon or mesoporous silica. They found that the addition of sucrose did not influence the final hexagonal mesoporous structure of silica but it lowered the pore ordering of the carbon material. They supposed that sucrose and its derivatives should locate at the interface between PEO and PPO segments of P123 copolymer under the synthesis condition [108,109]. Some sucrose molecules may interact with PEO segments and penetrate through the pores of the silica walls [108]. However, this synthetic pathway allows the incorporation of a quite limited amount of carbon precursor, *viz.* the sucrose to P123 molar ratio of 9.6 [109], to keep the micellar phases and their ordered packing. Otherwise, the resultant composite material may be disordered and wormhole-like, if the cylindrical P123 micelles are penetrated by excessive sucrose molecules or even separate carbon phase from sucrose can appear [109]. Polarz and co-workers observed the formation of a worm-type pore system when they used the supramolecular aggregates of nonionic ethyleneoxide-based surfactant and cyclodextrin as template for mesoporous silica synthesis [113]. Besides, the worm-like mesostructures from the macroscopic phase separation synthesis of phloroglucinol/formaldehyde/F127 can be assembled to more ordered hexagonal mesostructures through controlled solvent evaporation in films of the polymer-rich gel [62].

1.3. Dual hard and soft templating

Both hard and soft templates may be used at the same time for creating a bimodal porosity [114,115], making hollow nanospheres [116–118], improving synthesis efficiency [87,119], etc. Fan and co-workers achieved the synthesis of nanoporous carbon nanotubes through AAO (porous anodic aluminum oxide membrane) confined hydrogen-bonding self-assembly of PS-P4VP and sucrose during the

evaporation of dimethyl formamide [120]. Zhao and co-workers employed the 3D interconnecting struts of the poly(urethane) (PU) foam scaffold for the EISA process of phenolic resol/F27 [119] or resol/TEOS/F127 [87] synthesis solution. The PU foam not only provided a high surface area for solvent evaporation, but also generated a macroporous architecture after its decomposition [87,119]. Evaporation-induced organic-organic assembly of resol/F127 into mesostructures can also occur in the void of silica microspheres [114]. The macroscopic phase separation synthesis of resorcinol-formaldehyde/TEOS/F127 can be performed in the presence of silica microspheres [115]. The removal of silica species both resulted in bimodal porous carbon materials [114,115]. The above examples are all about involving a hard template during the soft-templated synthesis of mesoporous carbon or silica-carbon nanocomposites without influencing the assembly process. The soft-templating synthesis of mesoporous silica or organosilica hybrid can be conducted in the presence of a hard template as well. Yang and co-workers reported that a hollow mesostructured silica shell of *ca.* 50 nm can be synthesized with polystyrene spheres as hard template, on which TEOS and chlorosilane ($\text{Cl}_3\text{SiC}_8\text{H}_4\text{F}_{13}$ or $\text{Cl}_3\text{SiC}_8\text{H}_{17}$) co-condensed around CTAB micelles [117]. Similarly, when TEOS was co-condensed with poly(methacrylate)-organosilane (PMA-Si), hybrid mesoporous hollow nanospheres were formed [116]. Porous polymeric layer can also be prepared from dual hard and soft templating [118,121]. Huo and co-workers coated SiO_2 spheres with resorcinol-formaldehyde in the presence of CTAB *via* a modified Stöber reaction. After pyrolysis, *ca.* 0.6 nm wormlike micropores were uniformly distributed in the carbon shell (*ca.* 28 nm thick) [118]. Zhang and co-workers coated Si spheres with a porous carbon shell (15–20 nm thick with 3–5 nm pores) with glucose in the presence of F127 *via* a hydrothermal autoclaving process at 180 °C for 6 h [121].

2. Carbonization

The as-synthesized mesostructured carbon/template or silica-carbon/template composites from soft-template synthesis, need to be subjected to a thermal treatment (“carbonization”) to transform the carbon precursor to a carbon matrix and remove the template. Carbonization involves the reactions of dehydration, condensation, polymerization and aromatization of the carbon precursor. Generally, carbonization can be conducted in the form of pyrolysis and hydrothermal carbonization. With respect to the carbon precursor in the mesostructured carbon/template or silica-carbon/template composites, the carbonization may already occur in the synthesis step, such as in the hydrothermal autoclaving process, or in the extra thermal curing (thermopolymerization) step which strengthens the structure. As a suitable carbon precursor, it should have the propensity to polymerize and show the resistance to decomposition during the carbonization process [20,32]. Aromatic compounds, such as phenol-formaldehyde, and heteroaromatic compounds, such as furan derivatives from carbohydrates, are all suitable building blocks for carbonization. In addition, with the catalysis of acid, such as the non-volatile H_2SO_4 , the P123 copolymer [64,65] and even butanol [112] can act as the carbon source.

2.1. Pyrolysis

Pyrolysis is the process of thermal treatment under an inert atmosphere (N_2 , Ar). It is the most commonly adopted way for carbonization. Dai and co-workers pyrolyzed resorcinol-formaldehyde/PS-P4VP film from EISA synthesis in N_2 , and they observed the amorphous carbon pore wall from phenolic resin by Raman spectra and XRD patterns [63]. Similarly, Zhao and co-workers obtained an amorphous carbon framework after pyrolyzing the resol/Pluronic copolymer films from EISA synthesis [61,81]. Hara and co-workers studied the direct pyrolysis of natural organics such as sugars, starch and cellulose at different temperatures, and they observed the formation of small

polycyclic aromatic carbon sheets bearing phenolic OH and COOH groups by ^{13}C CP/MAS NMR [122–125]. Low pyrolysis temperatures (< *ca.* 250 °C) generates complex polymers containing aromatic compounds [122,123]. Clark and co-workers found that at this stage CH_2OH groups condense, coupled with glycosidic ring opening, to produce carbonyl groups conjugated with olefinic groups, generating aliphatic and alkene/aromatic functions [126,127]. With the increase of pyrolysis temperature (> 300 °C), the aliphatic groups are gradually converted to small graphene sheets with a full aromatic π systems comprising multiple fused aromatic rings [122,123,126,127]. These polycyclic aromatic carbon sheets grow larger with increasing pyrolysis temperature (> *ca.* 450 °C) (and time) and they become more hydrophobic, less flexible, higher cross-linked and closer stacked [122–124]. Lou and co-workers studied the incomplete carbonization of bagasse under N_2 flow at temperatures of 300–500 °C. They observed similar growth and stack of polycyclic aromatic carbon sheets, and the gradual reduction of OH and COOH groups by XRD patterns and FTIR spectra, respectively [128]. Anyway, the direct pyrolysis of biomass only produces carbonaceous materials with low surface areas (< $2 \text{ m}^2 \text{ g}^{-1}$), containing *ca.* 1 nm aromatic carbon sheets [122,125,129]. The functional groups of the carbon are determined inherently by the carbon precursor besides the pyrolysis temperature. Zhao and co-workers filled SBA-15 pores with sucrose, furfuryl alcohol, naphthalene and anthracene precursor [130]. They found that the use of sucrose and furfuryl alcohol can provide higher surface areas up to $1470 \text{ m}^2 \text{ g}^{-1}$ and abundant functional groups such as carboxyls, anhydrides, lactones, hydroxyl, carbonyl, etc. On the contrary, carbons from naphthalene and anthracene have a higher graphitization degree.

Though pyrolysis is a convenient way of transforming the carbon precursor and modifying the oxygenated groups of the carbon phase, organic-organic composites obtained by soft-templating synthesis may not preserve the well-ordered mesostructure during such pyrolysis. For example, the pyrolysis of resol/F127 composite can lead to a severe shrinkage of the framework [61,81], or even yield a disordered and collapsed porous structure [131,132]. At about 350 °C, the Pluronic copolymer template can be almost completely removed in N_2 [43]. With the degradation of the template during pyrolysis, the mesostructural stability is difficult to ensure while pores are opened. Zhao and co-workers proposed the removal of template by solvent extraction with the aid of 48 wt% H_2SO_4 instead of pyrolysis, but it needs refluxing for 24 h [81]. The introduction of silicate in the material appears promising to increase the thermo-stability of the mesoporous material [43,132]. The rigid silica constituent in the composite helps to reduce the framework shrinkage during pyrolysis, attributed to the reinforcement of the mechanical properties that lead to resistance to the stress-induced collapse of the mesostructure [43,81,132]. Due to the robust silica framework, mesoporous silica/carbon nanocomposites can be formed from the pyrolysis of organosilica/surfactant mesophases, such as ethane-bridged organosilica/CTAB [133] and phenyl-bridged organosilica/OTAB (octadecyltrimethylammonium bromide) [134]. Moreover, during the pyrolysis, the amorphous silica in the nanocomposite become more condensed and the silanol groups can have catalytic influence in reducing the oxygenated compounds of carbon phase [135].

2.2. Hydrothermal carbonization

A hydrothermal carbonization (HTC) typically at the temperature range of 130–250 °C in the subcritical aqueous media can be carried out instead of the dry pyrolysis [136,137]. The hydrothermal treatment is a well-established method to convert lignocellulosic biomass to more condensed functional materials, such as essentially nonporous carbon microspheres [136–144]. Compared to pyrolysis, this process emits minimum amount of greenhouse gases and the majority of the original carbon is incorporated into the final structure, *i.e.* a hydrochar [137]. The as-obtained hydrochar displays a core-shell structure composed of a hydrophobic core and a stabilizing hydrophilic shell that contains

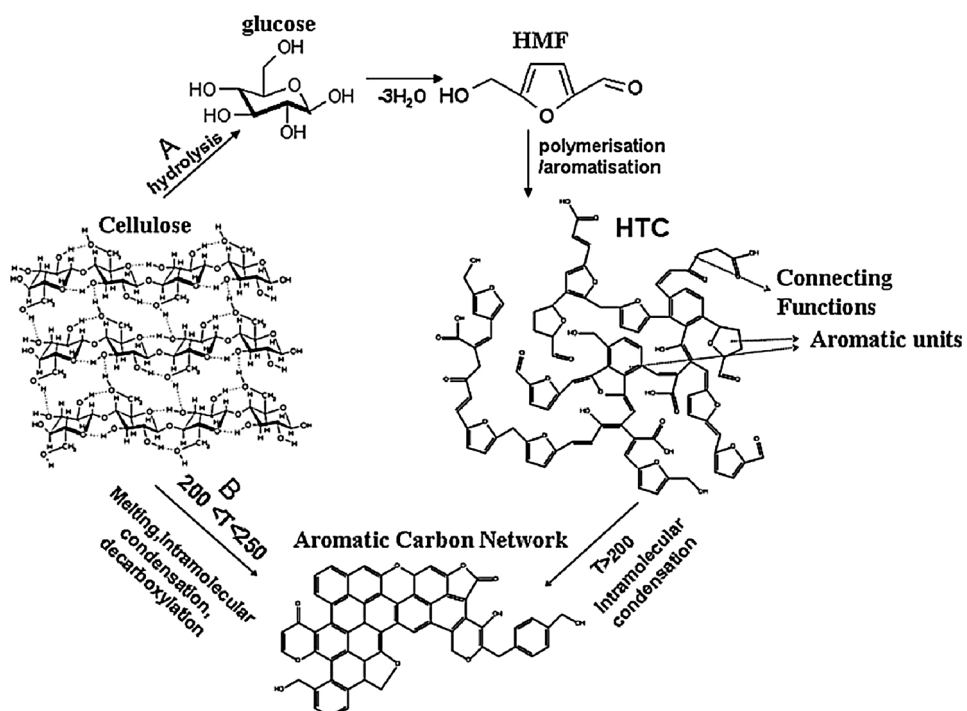


Fig. 6. Conversion of cellulose into hydrochar: (A) via HMF resulting in a furan-rich aromatic network and (B) direct aromatization. Reproduced with permission from Ref. [136]. Copyright 2012 Royal Society of Chemistry.

abundant oxygen functional groups (hydroxyl, phenolic, carbonyl and carboxyl groups) [136,138,143]. The hydrothermal carbonization method has the specific advantage of generating functional groups, due to the long residence time of intermediates, the presence of H_2O and pressure, etc. [137,145]. The formation mechanism is shown in Fig. 6 [136,138]. The second model in the graph emphasizes the direct formation of a polyaromatic carbon network, while the first model highlights the intermediate formation of polyfuranic carbon network [136,138]. Baccile and co-workers found by ^{13}C solid-state CP/MAS NMR that irrespective of the nature of hexose sugar, similar carbon materials were produced, but they were different from those from pentose sugars [142]. These results demonstrated the formation of cross-linked furan-based structures during HTC from HMF for hexoses, or from furfural for pentoses.

The hydrothermal synthesis has been coupled to the template-mediated synthesis of carbon or silica-carbon nanocomposites [60,136]. For soft-templating, this has been discussed in 1.2.4. For hard-templates, like silica beads and alumina membrane, the carbonaceous coating can be formed by simply adding the template into the aqueous solution of carbon precursor followed by hydrothermal autoclaving treatment [60]. For the templates like calcined SBA-15 [145] and meso-macroporous silica monolith [146], the silica pores are firstly infiltrated with liquid containing carbon precursor and then placed in the closed autoclave. However, the polymer-like furan-rich carbon structure from HTC is too “soft” and easily crashes after the removal of silica template [146]. A HTC process is usually followed by further pyrolysis to stabilize the carbon skeleton and to create a porous structure [145,146].

Recently, we proposed a novel vapor-phase assisted HTC procedure at 200 °C to derive carbonaceous materials from carbohydrate precursors [267]. The physical separation of liquid phase water and the contact with vapor phase water result in carbons with appreciable mesoporosity in contrast to the nonporous counterpart from conventional HTC, but with similar abundance in surface oxygenates (i.e. COOH and phenolic OH groups).

3. Sulfonation

Mesoporous carbon or silica-carbon nanocomposites can be functionalized with SO_3H to become SO_3H bearing (sulfonated) mesoporous carbon or silica-carbon solid acid catalysts. A significant number of acid-catalyzed reactions, such as esterification, hydrolysis, dehydration and Friedel-Crafts condensation reactions, are still carried out using homogeneous acid, such as H_2SO_4 . The homogeneous acid catalysis imposes problems of waste water production, equipment corrosion, difficult product purification, etc. Solid acid catalysts are much more environmentally friendly owing to the easy recovery and reusability [147]. Cation-exchange resins (SO_3H resins), such as cross-linked polystyrene-based sulfonic acids (Amberlyst and Dowex) and perfluorosulfonic acid-based polymer (Nafion), have been utilized as solid acid catalysts which exhibit good performance for various acid-catalyzed reactions, with the strong acid strength and high acid density [10,147,148]. However, the accessibility to the acid sites is limited, due to the low surface area ($< 50 \text{ m}^2 \text{ g}^{-1}$) for the macroporous structure of the resins [10,147]. Moreover, due to their low thermal and hydrothermal stability, these SO_3H resins are limited to low temperature uses [149]. For example, the operation temperature of Amberlyst-15 is below 120 °C. A more appealing class of solid acids is sulfonated mesoporous carbon or silica-carbon nanocomposites, not only due to their strong acidity and well-ordered mesostructure, but also due to the H_2O -tolerant nature, which is ascribed to the carbon moieties in the framework from either pyrolysis or hydrothermal treatment. The incorporation of chemically bound SO_3H groups can be roughly divided into built-in and post-grafting approaches, as summarized in Fig. 7. Brief comments for each sulfonation approach and some of the sulfonated carbon or silica-carbon nanocomposite based acid catalysts reviewed in this section are presented in Table 1.

3.1. Built-in approach

3.1.1. Using TsOH as sulfur and carbon source

The built-in approach refers to the use of SO_3H or SH containing precursor for the formation of the material. The most commonly used

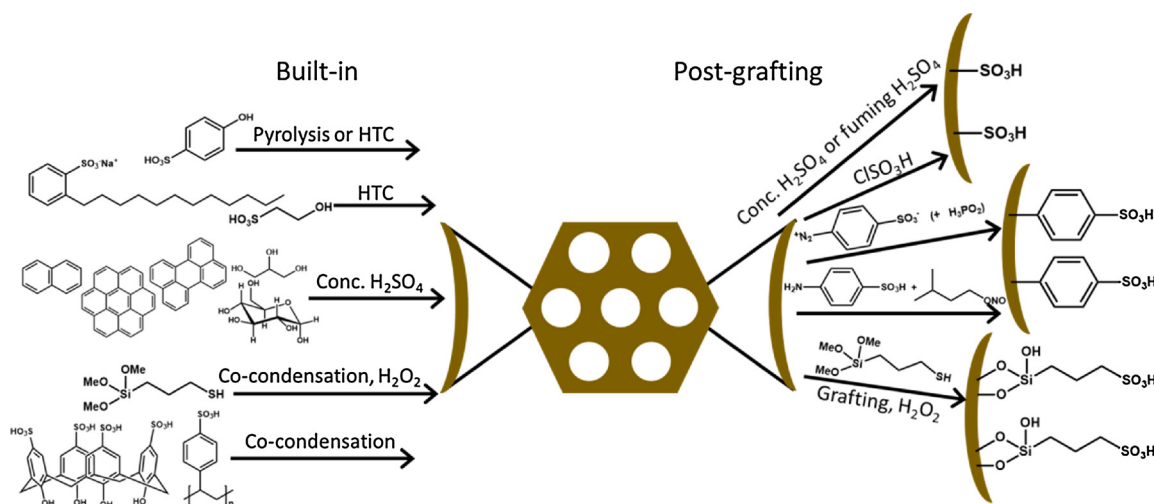


Fig. 7. Summary of possible ways that permit functionalization of the surface of mesoporous carbon or silica-carbon nanocomposites with C-SO₃H groups.

sulfur source is *p*-toluenesulfonic acid (TsOH), which is simultaneously a carbon precursor [40,45,150–152]. Valente and co-workers used pyrolyzed TsOH at 250 °C with the addition of H₂SO₄ as activating agent under the hard templating of silica [40] or fuming SiO₂ [45]. They obtained sulfonated mesoporous silica-carbon nanocomposites with SO₃H density of 0.8–2.2 mmol/g, which effectively catalyzed the conversion of HMF in ethanol [40]. Wang and co-workers mixed TsOH and glucose and after hydrothermal autoclaving at 180 °C for 24 h, they obtained a sulfonated carbonaceous catalyst with 1.3 mmol/g SO₃H for the dehydration of fructose [152] and esterification of succinic acid [151]. TsOH, glucose and resorcinol were mixed for the hydrothermal carbonization to produce carbonaceous monolith with *ca.* 1.4 mmol/g SO₃H for the acetalization reaction of benzaldehyde [150]. Sodium dodecylbenzene sulfonate [153] and hydroxyethylsulfonic acid [154] were also applied for the hydrothermal carbonization together with furfural for producing carbonaceous material with SO₃H of 1.1 [153] and 2.4 [154] mmol/g, respectively, for esterification reactions. The introduction of the long carbon chains provide hydrophobic domains that facilitate the esterification of bulky organic acids like pivalic acid [153].

3.1.2. One-pot sulfonation and carbonization by concentrated H₂SO₄

The direct treatment of carbon precursor with concentrated H₂SO₄ can produce carbonaceous material functionalized with SO₃H. Hara and co-workers heated aromatic compounds such as naphthalene, perylene and coronene in concentrated H₂SO₄ at 250 °C for 15 h for the one-step formation and incomplete carbonization of sulfoaromatic hydrocarbons [155]. The SO₃H acid density of the obtained solid is as high as 4.9 mmol/g [155]. However, this method is highly dangerous and the sulfopolycyclic aromatic hydrocarbons are leached from the solid by liquid-phase reactions over 100 °C or with higher fatty acids as surfactants [156]. Glucose was sealed in autoclaves with concentrated H₂SO₄ and heated at 180 °C for 24 h [151,157]. The SO₃H density is 1.35 [151] or 0.91 [157] mmol/g, which is comparable to the solid acid synthesized from glucose and TsOH under the same condition [151,152]. However, due to the more hydrophilic surface, the selectivity for the esterification product of succinic acid and ethanol is much lower [151]. Hydrothermal autoclaving treatment at 180 °C of glycerol and concentrated H₂SO₄ also produced polycyclic aromatic carbon based solid acid with 1.03 mmol/g SO₃H, which showed high catalytic performance in the esterification reaction of oleic acid with methanol [158]. Viswanadham and co-workers slowly added concentrated H₂SO₄ to the mixture of glucose and TEOS, leading to the formation of sulfonated silica-carbon composite gel [159,160]. After subjecting to hydrothermal curing (autoclaving at 150 °C for 15 h) and

pyrolysis (under N₂ at 300 °C for 4 h), the obtained material has only 0.07 mmol/g SO₃H but it is quite stable for glycerol acetalization reaction with acetone [160]. The relatively low SO₃H density is probably due to the decomposition of sulfonated carbon at temperature > 250 °C [155,161], and in the sulfonated silica-carbon composites, the decomposition may start at an even lower temperature [38].

3.1.3. Co-condensation with S-containing organosilanes

For organosilica hybrids, the incorporation of SO₃H typically involves the co-condensation of TEOS with organosilanes carrying S-containing terminal groups [22–25]. Riisager and co-workers reported the synthesis of propyl-SO₃H functionalized SBA-15, through the co-condensation of 3-mercaptopropyltrimethoxysilane (MPTMS) with TEOS in the presence of P123 [162]. The as-obtained thiol-functionalized silica was washed by HCl-ethanol solution under refluxing and oxidized by H₂O₂ for the catalytic conversion of fructose to ethyl levulinate (EL) [162]. Employing a similar method, Dumesic and co-workers prepared propyl-SO₃H functionalized organosilicas with different amount of ethane linkers in the mesostructure, which showed steady catalytic activity for fructose dehydration reaction [163]. Melero and co-workers synthesized arene-SO₃H functionalized mesoporous organosilicas by using 2-(4-chlorosulfonylphenyl)-ethyl-trimethoxysilane (CSPTMS) as an alternative S precursor [164]. The arene- and propyl-SO₃H functionalized mesoporous organosilicas from co-condensation synthesis had *ca.* 0.9 mmol/g of SO₃H and the inherent acid strength of alkyl-SO₃H is lower than arene-SO₃H, but propyl-SO₃H showed higher catalytic activity for the esterification of vanillyl alcohol and hexanol due to the more hydrophobic local environment [164,165].

Due to the hydrophobic nature of the silane reagents, the silica walls were functionalized only by a limited amount of SO₃H groups through co-condensation [24]. In the self-assembly condensation of MPTMS and TEOS, the amount of MPTMS is restricted to a molar content of 33% in the total silicate sources, corresponding to 2.73 mmol/g S [166]. Wan and co-workers alternatively employed MPTMS in the soft-templating synthesis of resol/TEOS/F127 via multi-constituent EISA approach for ordered mesoporous SH-functionalized hybrid material [166,167]. MPTMS cannot replace TEOS in the co-assembly with resol and F127, due to the 3-connected Si–O bonds in MPTMS. In contrast, it disturbed the co-assembly of resol, TEOS and F127, since it disrupted the cross-linking of 4-connected TEOS to form rigid SiO₂ framework, though it can also form Si–O–C bonds with resol, which led to the enhancement of the MPTMS loading up to 3.79 mmol/g [166]. Followed by extraction with 48 wt% H₂SO₄ at 90 °C for 24 h and oxidation with H₂O₂, sulfonated mesoporous silica-carbon nanocomposite with 2.38 mmol/g

Table 1
Different routes of introducing SO_3H groups into carbon or silica–carbon nanocomposites and examples as catalysts for a wide variety of acid-catalyzed reactions.

Sulfonation methodology	Remarks ^a	Example	Preparation procedure	S_{BET} (m^2/g)	^b (mmol/g)	Reaction	Stability	Ref.	
Built-in	Using TsOH as sulfur and carbon source	Expensive and possibly poor porosity, but the SO_3H density and surface properties is controllable at the very start	HTC-MC-1.25-2	Mixture of TsOH , glucose and resorcinol, hydrothermally carbonized at 180 °C	97	1.39	Acetalization of benzaldehyde with methanol	Decreased to 77% of the initial conversion of benzaldehyde after 4 runs, due to S leaching	[150]
			Glu-TsOH	Mixture of TsOH and glucose, hydrothermally carbonized at 180 °C	< 1	1.27	Esterification of succinic acid with ethanol	Decreased to 33% of the initial selectivity of diethyl succinate after 4 runs, due to the changes in surface chemistry	[151]
			F-T	Mixture of TsOH and furfural, hydrothermally carbonized at 180 °C	34	1.2	Esterification of pivalic acid with methanol	Not reported	[153]
			F-S	Mixture of sodium dodecylbenzene sulfonate, furfural and a little H_2SO_4 , hydrothermally carbonized at 180 °C	40	1.1		Good stability for 5 runs	[153]
			Carbonaceous material	Mixture of hydroxyethylsulfonic acid and furfural, hydrothermally carbonized at 180 °C	148	2.4	Esterification of acetic acid with butanol; Oxathiolketalization of cyclohexanone with mercaptoethanol	Stable for both reaction for 4 runs	[154]
				⁵²⁶			Esterification of succinic acid with ethanol	Not reported	[151]
							Esterification of acetic acid with ethanol	Stable with the regeneration by acetone washing and heating at 200 °C in air	[157]
							Dehydration of phenylethanol	Stable for the esterification reaction	[155]
One-pot sulfonation and carbonization by concentrated H_2SO_4	Cheap and simple, but rigorous, and the resulting carbon network may be unstable.	⁵²⁶	$\text{Glu-SO}_3\text{H}$	Glucose hydrothermally sulfonated and carbonized in concentrated H_2SO_4 at 180 °C	< 1	1.35			
			S-Dg	Glucose hydrothermally sulfonated and carbonized in concentrated H_2SO_4 at 180 °C	3.9	0.91			
			Carbon-based solid acid	Naphthalene sulfonated and carbonized in concentrated H_2SO_4 at 250 °C	24	4.90	Esterification of acetic acid with ethanol; Hydrolysis of cyclohexyl acetate; Hydration of 2,3-dimethyl-2-butene		
			SCS	Mixture of glucose and TEOS, sulfonated and carbonized in concentrated H_2SO_4 , pyrolyzed at 300 °C	780	0.11	Alkylation of phenol with tertiary butyl alcohol	Stable	[159–160]
			HSCl/2	Mixture of glucose and TEOS, sulfonated and carbonized in concentrated H_2SO_4 , hydrothermally carbonized at 150 °C and pyrolyzed at 300 °C.	242	0.07	Acetalization of glycerol with acetone	Stable	[160]
Co-condensation with S-containing organosilanes	Expensive, but the stability is improved with the stable Si–C bonds.	Propyl- SO_3H -SBA-15					Etherification of vanillyl alcohol with 1-hexanol	Not reported	[164]
		Arene- SO_3H -SBA-15						Not reported	[164]

(continued on next page)

Table 1 (continued)

Sulfonation methodology	Remarks ^a	Example	Preparation procedure	S_{BET} (m^2/g)	^b (mmol/g)	Reaction	Stability	Ref.
		Co-condensation of TEOS and CSPTMS in the presence of p123, removal of P123 and oxidized by H_2O_2				Condensation of phenol with acetone; Acetalization of 1,4-butanediol with butyraldehyde	Good stability for 20 runs, with only slight S leaching	[167]
		MP-SO ₃ H-27.4	448	2.38		Dehydration of xylose to furfural	Deactivated during the first run due to polymer leaching, but stable for the next 2 runs	[169]
Using other S-containing precursors	The S-containing precursors like poly(styrene sulphonic acid) needs to be synthesized beforehand, and the attachment to the catalyst may be unstable. Cheap, but harsh and corrosive with side reactions like oxidation, dehydration, cross-linking, etc., needs an elevated temperature and often destroys the mesoporous structure	Si-PSSA-50.1	PSSA was added to the sol of TEOS and 3-aminopropyltriethoxysilane at 100 °C	59	1.5			
Post-grafting	Concentrated H_2SO_4 or fuming H_2SO_4	Sulfonated carbon	Glucose pyrolyzed at 400 °C and sulfonated in concentrated H_2SO_4	2	0.75	Hydration of 2,3-dimethyl-2-butene; Esterification of acetic acid with ethanol	Stable	[123]
		C400-SO ₃ H	Glucose pyrolyzed at 400 °C and sulfonated in concentrated H_2SO_4	< 1	0.64	Esterification of acetic acid with methanol; Transesterification of triacetin	Deactivation due to leaching of sulfonic groups-containing polyaromatic species	[171]
		FDU-15-50-180	Soft-template synthesis of P127/phenol-formaldehyde, pyrolyzed at 500 °C and sulfonated in concentrated H_2SO_4	393	1.71	Condensation of phenol with acetone	Not reported	[173]
		FDU-14-SO ₃ H	Soft-template synthesis of P123/phenol-formaldehyde, pyrolyzed at 350 °C and sulfonated in contact with the vapor of 50% $\text{SO}_3/\text{H}_2\text{SO}_4$	539	2.2	Beckmann rearrangement of cyclohexanone oxime; Acetalization of benzaldehyde or 1-pyrenecarboxaldehyde with ethylene glycol	Stable for both reactions with the regeneration of washing by dilute H_2SO_4 and boiling H_2O	[178]
		CMK-3-823-SO ₃ H	Hard-template synthesis with SBA-15 and sucrose, pyrolyzed at 550 °C, removal of SiO_2 and sulfonated in contact with the vapor of 50% $\text{SO}_3/\text{H}_2\text{SO}_4$	1187	1.2		Stable for Beckmann rearrangement with the regeneration of washing by 5 wt% H_2SO_4 and hot H_2O .	[179]
		Ph-SO ₃ H HME	Condensation synthesis of bis (triethoxysilyl)ethylene in the presence of P123, washed by HCl and EtOH, modified by benzocyclobutene and sulfonated in concentrated H_2SO_4	565	1.44	Esterification of acetic acid; Pinacol-pinacolone rearrangement	Stable for the esterification reaction	[180]
	carbon (20 wt %)/SBA-15		Hard-template synthesis with SBA-15 and sucrose, pyrolyzed at 550 °C and sulfonated in concentrated H_2SO_4	723	0.13	Dimerization of α -methylstyrene	Stable	[41]
MC-1.2				724	0.46	Esterification of acetic acid with <i>n</i> -butyl alcohol		[183]

(continued on next page)

Table 1 (continued)

Sulfonation methodology	Remarks ^a	Example	Catalyst	Preparation procedure	S_{BET} (m^2/g)	^b (mmol/g)	Reaction	Stability	Ref.
ClSO_3H	Expensive, functions at 0 °C, beneficial for retaining the structure, but could form other bonds like Si-O-SO ₃ H aside from C-SO ₃ H and evolve corrosive HCl	PS-SO ₃ H/ 2.5PMA-Si- H_2SO_4	Hard-template synthesis with MCM-48 and sucrose, pyrolyzed at 400 °C and sulfonated in concentrated H ₂ SO ₄					MCM-48 from the calcination of the spent catalyst, can be used for the preparation of MC-1.2 again, showing the same activity	[116]
$\text{HSC-SO}_3\text{H}$	Expensive and toxic, but stable and occurs at low temperature by use of <i>in-situ</i> generated benzenesulfonic acid containing aryl radicals, beneficial for retaining the mesoporous structure	PS-SO ₃ H/ 2.5PMA-C8- SiO_2	Dual-template synthesis with PS nanospheres, and PMA-Si and TEOS in the presence of CTAB, washed by HCl and EtOH, treated by THF, sulfonated using ClSO ₃ H	128	1.9	Esterification of lauric acid with ethanol	Deactivated due to leaching of the active acidic sites	[116]	
$\text{HSC-SO}_3\text{H}$	Expensive and toxic, but stable and occurs at low temperature by use of <i>in-situ</i> generated benzenesulfonic acid containing aryl radicals, beneficial for retaining the mesoporous structure	PS-SO ₃ H/ 2.5PMA-C8- SiO_2	Dual-template synthesis with PS nanospheres, and PMA-Si and TEOS in the presence of CTAB, modified by octyltriethoxysilane, washed by HCl and EtOH, treated by THF, sulfonated using ClSO ₃ H	115	1.8	Good stability for 10 runs			
$\text{HSC-SO}_3\text{H}$	Expensive and toxic, but stable and occurs at low temperature by use of <i>in-situ</i> generated benzenesulfonic acid containing aryl radicals, beneficial for retaining the mesoporous structure	PS-SO ₃ H/C ₈ - SiO_2 -0.10	Dual-template synthesis with PS nanospheres, and <i>n</i> -octyltrichlorosilane and TEOS in the presence of CTAB, washed by HCl and EtOH, treated by THF, sulfonated using ClSO ₃ H	222	1.13	Esterification of lauric acid with ethanol; Transesterification of tripalmitin with methanol	Good stability for esterification reaction for 10 runs, with the combined effect of PS-SO ₃ H swelling and decrease in surface area	[117]	
$\text{HSC-SO}_3\text{H}$	Expensive and toxic, but stable and occurs at low temperature by use of <i>in-situ</i> generated benzenesulfonic acid containing aryl radicals, beneficial for retaining the mesoporous structure	CMK-5-PSA	Hand-template synthesis with as-formed SiO ₂ (from TEOS) and resorcinol-formaldehyde, removal of SiO ₂ , sulfonated using ClSO ₃ H	419	1.9	Acetalization of glycerol with acetone	Stable for 4 runs	[187]	
$\text{HSC-SO}_3\text{H}$	Expensive and toxic, but stable and occurs at low temperature by use of <i>in-situ</i> generated benzenesulfonic acid containing aryl radicals, beneficial for retaining the mesoporous structure	AC-SO ₃ H	Hand-template synthesis with SBA-15 and furfuryl alcohol, pyrolyzed at 1000 °C, removal of SiO ₂ , sulfonated using 4-benzene-diazoniumsulfonate (from sulfanilic acid and NaNO ₂) at 3–5 °C	616	0.90	Dehydration of fructose in the flowing THF-water	Slightly deactivated due to the slow hydrolysis of C-SO ₃ H	[189]	
$\text{ArSO}_3\text{H-}$ HMCS3.2-1	Expensive and toxic, but stable and occurs at low temperature by use of <i>in-situ</i> generated benzenesulfonic acid containing aryl radicals, beneficial for retaining the mesoporous structure		Activated carbon, sulfonated using 4-benzene-diazoniumsulfonate (from sulfanilic acid and NaNO ₂) and H ₃ PO ₂ at 0–5 °C	602	0.90	Esterification of acetic acid, hexanoic acid or decanoic acid with ethanol	Deactivated due to leaching of SO ₃ H groups, though regenerated by washing with 1 mol/L H ₂ SO ₄	[192]	
CMK-5-SO ₃ H	Expensive and toxic, but stable and occurs at low temperature by use of <i>in-situ</i> generated benzenesulfonic acid containing aryl radicals, beneficial for retaining the mesoporous structure		Hand-template synthesis with SMCS-Al-1 ^c and furfuryl alcohol, pyrolyzed at 800 °C, removal of template, sulfonated using 4-benzene-diazoniumsulfonate (from sulfanilic acid and isocyanohydrite) at 30 °C	418	0.86	Esterification of levulinic acid with ethanol; Ethanolysis of furfuryl alcohol; Hydrolysis of ethyl benzoate	Stable for the esterification and hydrolysis reactions	[193]	
				843	1.93			[195]	

(continued on next page)

Table 1 (continued)

Sulfonation methodology	Remarks ^a	Example	Preparation procedure	S_{BET} (m^2/g)	b (mmol/g)	Reaction	Stability	Ref.
SH or SO_3H terminated organosilanes	Expensive and based on surface silylation the density of acid sites is limited, but with subtle modification to the structure	$\text{O-Si}(\text{CH}_2)_2\text{-Ar-SO}_3\text{H}$	Hard-template synthesis with Al-SBA-15 and furfuryl alcohol, pyrolyzed at 850 °C, removal of SiO_2 , sulfonated using 4-benzene-diazoniumsulfonate (from sulfanilic acid and NaNO_2) and H_2PO_2 at 5 °C	Not reported	0.62	Transesterification of triolein with methanol	Stable for 4 runs	[198]
		$-\text{O-Si}(\text{CH}_2)_3\text{-SO}_3\text{H}$	Carbon nanofibers, sulfonated using 4-benzene-diazoniumsulfonate (from sulfanilic acid and isocyanogenitrile) at 30 °C, MCM-41 grafted with MPTMS and oxidized by H_2O_2	493	0.4	Dehydration of xylose	Deactivated due to inefficient removal of adsorbed by-products on the catalyst surface	[201]
			Soft-template synthesis of FI27/phenol-formaldehyde, pyrolyzed at 400 °C, sulfonated (or silylated) by 2-(4-chlorosulfonylphenyl)ethyl trichlorosilane	425	0.52	Esterification of <i>n</i> -propanol with acetic acid; Asymmetric Adol condensation of 2-butanone with 4-(trifluoromethyl)benzaldehyde	Deactivated in the esterification reaction, due to leaching of the acid groups	[202]
			soft-template synthesis of FI27/phenol-formaldehyde, pyrolyzed at 400 °C, sulfonated (or silylated) by MPTMS, oxidized by H_2O_2	428	0.74	Deactivated in the esterification reaction, but less severe than the aromatic sulfonated material		

^a Brief remarks on the advantages and disadvantages of each sulfonation method.^b Represents the SO_3H group density in the catalyst.^c Prepared by co-condensation of TEOS, octadecyltrimethoxysilane and $\text{Al}_2(\text{SO}_4)_3$ on the as-formed SiO_2 nanospheres (from TEOS), followed by calcination in air at 550 °C.

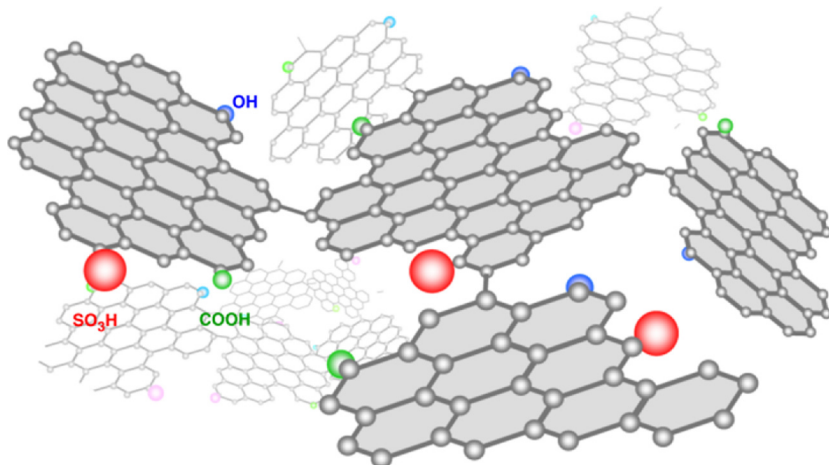


Fig. 8. Schematic structure of partially carbonized carbohydrate after sulfonation. Reproduced with permission from Ref. [125]. Copyright 2007 American Ceramic Society.

SO_3H was obtained, which showed high catalytic activity in the condensation of phenol and acetone, and acetalization of 1,4-butanediol and butyraldehyde [167].

3.1.4. Using other S-containing precursors

There are many other S-containing precursors that have the possibility to be introduced into the synthesis of mesoporous carbon or silica-carbon nanocomposites. For example, Fernandes and co-workers reported the synthesis of *p*- SO_3H calixarene-functionalized alkyl-bridged organosilica through a sol-gel process by simply adding the SO_3H -calixarene to TEOS in the presence of HCl [168]. This SO_3H functionalized solid catalyst (0.32 mmol/g SO_3H) showed high activity towards the esterification reaction of palmitic acid with ethanol [168]. Lopez Granados and co-workers started from TEOS, 3-aminopropyl triethoxysilane (APTES) and poly(styrene sulfonic acid) (PSSA) to prepare silica-PSSA nanocomposite through a sol-gel route [169]. The polymer was incorporated into the silica particle network through SO_3^- - NH_3^+ electrostatic interaction and the resultant composite was microporous with 1.5 mmol/g SO_3H and catalyzed the dehydration of xylose to furfural [169].

Though the build-in method is straightforward and the amount of SO_3H can be tuned by adjusting the amount of S precursor, in general, this method is difficult to couple with soft-templating synthesis, not only due to the limited thermal stability of C–S O_3H moieties, but also due to the influence of the S precursor in the construction of the micellar mesophase. As a consequence, a post-synthetic grafting approach is more frequently applied.

3.2. Post-grafting approach

The possible post-grafting approaches of functionalizing mesoporous carbon or silica-carbon nanocomposites with SO_3H groups involve the use of various sulfonating reagents, as listed in Fig. 7. The key point in post-grafting is the preservation of the original mesostructure, while incorporating as many SO_3H groups as possible.

3.2.1. Concentrated H_2SO_4 or fuming H_2SO_4

In 2005, Hara and co-workers firstly proposed the sulfonation of partially carbonized carbohydrate in concentrated H_2SO_4 at an elevated temperature (e.g. at 150 °C) under N_2 [170]. The resultant amorphous carbon is composed of flexible polycyclic aromatic carbonaceous sheets bearing OH, COOH and high density of SO_3H groups in a 3D sp^3 -bonded structure, as shown in Fig. 8 [123,125,129,170]. As discussed in 2.1, with the raise of pyrolysis temperature, the organic material transforms from aromatic-containing polymers to small and loose polycyclic aromatic carbon sheets, and to larger and denser graphitic carbon rings

with reducing aromaticity [122–124]. Consequently, the sulfonation of carbon, pyrolyzed at low temperatures (< ca. 250 °C), will produce a lot of soluble sulfonated species, while the sulfonation of carbon, pyrolyzed at high temperatures (> ca. 450 °C), will produce more stable sulfonated carbon but with a low amount of SO_3H [122]. Moreover, the co-existing OH and COOH groups increase the sulfonation efficiency [49,161]. An optimum pyrolysis temperature at ca. 400 °C was found for glucose [123], cellulose [124], and bagasse [128] with SO_3H density of 0.7, 1.8 (using fuming H_2SO_4) and 1.1 mmol/g, respectively after sulfonation. The use of fuming H_2SO_4 can increase the SO_3H amount on the 400 °C pyrolyzed glucose to 1.3 mmol/g [123]. The duration of the pyrolysis process was found to have marginal influence [128,171]. As for hydrochar, the hydrothermal carbonization temperature mainly controlled the particle size [136]. The smaller particles formed at a lower hydrothermal temperature will be easily lost during the sulfonation and washing process, but the resulting SO_3H contents were all ca. 0.7 mmol/g for the 225, 245, 265 °C-hydrothermally treated cellulose after sulfonation by concentrated H_2SO_4 [144]. The application of fuming H_2SO_4 can result in 1.86 mmol/g SO_3H density for the 180 °C-hydrothermally treated glucose [140].

During the sulfonation process in concentrated H_2SO_4 , aside from the main electrophilic substitution reaction of introducing SO_3H , *viz.* $\text{Ar-H} + \text{H}_2\text{SO}_4 \rightarrow \text{ArSO}_3\text{H} + \text{H}_2\text{O}$, many side reactions may also occur in the carbonaceous material, such as oxidation, dehydration, condensation and cross-linking, *etc.* [155,171,172]. The influence of sulfonation conditions (temperature and time) on the properties of final carbonaceous sulfonated solid has also been investigated [128,161,173,174]. Depending on the type of carbon, the optimal sulfonation temperature is different; 150 °C, 180 °C and 250 °C were found to be the optimum sulfonation temperature respectively for 375 °C-pyrolyzed bagasse (1.06 mmol/g SO_3H) [128], 500 °C-pyrolyzed mesoporous carbon from EISA synthesis of resol/F127 (1.71 mmol/g SO_3H) [173] and active carbon (0.24 mmol/g SO_3H) [161]. The raise of sulfonation temperature can increase the hydrophilicity, [161] cause further carbonization (> 150 °C) [128], destroy the porous structure (> 180 °C) [173,175], and even decompose the sulfonate moiety (> 250 °C) [161]. The optimal sulfonation time was found to be 15 h [128,174]. The sulfonation process can be carried out in a Teflon-sealed autoclave (hydrothermal sulfonation), which is safer and easier, instead of in a flask under N_2 atmosphere [49,94,139,173,176,177].

The sulfonation of mesoporous carbon with concentrated H_2SO_4 or fuming H_2SO_4 will lead to a deterioration or even a severe collapse in the mesostructure [37,94,173,175,176,178,179]. Wu and co-workers reported a vapour-phase transfer method to synthesize SO_3H functionalized mesoporous carbons, *viz.* CMK-3 from hard-templating and FDU from soft-templating synthesis [178,179]. Careful sulfonation of the

samples was carried out through a gas-solid reaction, in which the sample powders were contacted with the vapour coming from a 50% $\text{SO}_3/\text{H}_2\text{SO}_4$ solution. This method is basically non-destructive in terms of textual properties of mesoporous carbon and the SO_3H density can be as high as 1.2 mmol/g for CMK-3 [178,179]. However, the use of toxic and volatile 50% $\text{SO}_3/\text{H}_2\text{SO}_4$ is adverse for operation.

Besides using other sulfonation agents at a relatively low temperature, as will be mentioned below, the incorporation of silica component in the mesostructure will largely reduce the structural influence by sulfonation [37,176]. Kondo and co-workers modified the mesoporous ethylene-bridged organosilica through a Diels-Alder reaction with benzocyclobutene [180]. The obtained phenylene-modified hybrid can be subjected to the sulfonation in concentrated H_2SO_4 and maintained its well-ordered mesoporous structure [180]. Benzene-bridged organosilica mesocellular foam (0.95 mmol/g SO_3H loading) [181] and benzene-bridged mesoporous organosilica (0.64 mmol/g SO_3H loading) [182] also maintained the porous structures, while being sulfonated by refluxing in concentrated H_2SO_4 .

Hard-templated mesoporous silica-carbon nanocomposites that are prepared by impregnating carbon precursor such as glucose [41], sucrose [183] and 2,3-dihydroxynaphthalene [38]) in silica mesopores, followed by pyrolysis, can also survive the direct sulfonation in concentrated H_2SO_4 [38,41,183]. The sulfonation may result in a slight increase of surface area and pore volume compared to the non-sulfonated composite, due to the side reactions like oxidation during the sulfonation procedure [38]. However, due to the drawbacks of hard-templating synthesis and the weight contribution from SiO_2 , the SO_3H density in these sulfonated silica-carbon nanocomposites was only 0.11–0.51 mmol/g [38,41,183]. Meanwhile, the silica template serves as a barrier for H_2SO_4 from reaching the carbon phase, especially in the case of fully impregnated silica-carbon composites, resulting in a rather low SO_3H content (0.39 mmol/g) for the mesoporous carbon after the silica removal [37,176,179]. Soft-templated mesoporous silica-carbon nanocomposites can to some extent avoid the problems met with hard-templating method during sulfonation. Sels and co-workers subjected the mesoporous silica-carbon nanocomposites via the EISA synthesis of sucrose/TEOS/F127 to the hydrothermal sulfonation in concentrated H_2SO_4 . The SO_3H density in the sulfonated nanocomposites can be tuned from 0.15 up to 0.57 mmol/g [68].

3.2.2. ClSO_3H

ClSO_3H is a much stronger sulfonation agent than concentrated H_2SO_4 and fuming H_2SO_4 . The sulfonation with ClSO_3H is normally carried out at room temperature [184–186] or 0 °C [116,117,187,188]. The room temperature treatment with ClSO_3H , even sulfonates the silanol groups into silica sulfuric acid [186]. At 0 °C, cellulose can be sulfonated by ClSO_3H to be cellulose sulfuric acid with 0.54 mmol/g SO_3H [188]. However, the oxygen-mediated anchoring in the sulfate groups is highly susceptible to hydrolysis and this leads to easy loss of acid sites [189]. On the other hand, Yang and co-workers prepared nanospheres of polystyrene core with a mesoporous organosilica hybrid shell [116,117]. Some polystyrene chains were entrapped in the mesochannels of the silica shell during the dissolution by THF, and the benzene rings of these polystyrene chains can be sulfonated by ClSO_3H at 0 °C, which gave 0.9–2.0 mmol/g SO_3H . The material showed a high activity and considerable stability for lauric acid esterification with ethanol [116,117]. Xiao and co-workers prepared nanospheres of SiO_2 core with resorcinol-formaldehyde resin shell [187]. After pyrolysis at 650 °C, etching by HF and treating with ClSO_3H at 0 °C, the microporous thin carbon shell with SO_3H (1.9 mmol/g) showed high performance in the acetalization of glycerol with acetone [187]. The hydrothermally coated carbon layers from hydrothermal carbonization of glucose in the presence of Fe_3O_4 nanoparticles can also be sulfonated by ClSO_3H to be functionalized with 1.4 mmol/g SO_3H . This carbon showed activity for the one-pot conversion of fructose and inulin into 5-ethoxymethylfurfural (EMF) [185]. The low temperature sulfonation

with ClSO_3H can anchor SO_3H through C–S and hardly influences the structure of the material, but the evolved by-product HCl may create serious problems in the industrial processing.

3.2.3. 4-benzene-diazoniumsulfonate

Another low temperature sulfonation method is the use of SO_3H -containing aryl radicals, which are generated from diazonium salts such as 4-benzene-diazoniumsulfonate [53,189–199]. Feng and co-workers reported the preparation of 4-sulfophenyl functionalized ordered mesoporous carbon by reacting CMK-5 with 4-benzene-diazoniumsulfonate in the presence of H_3PO_2 at 5 °C [194,195]. CMK-5 was prepared by using Al-SBA-15 as hard template and furfuryl alcohol as the carbon precursor after carbonization at 850 °C and removal of the hard template. The diazoniumsulfonate was prepared by the diazotization of 4-aminobenzenesulfonic acid with NaNO_2 . The aryl SO_3H functionalized mesoporous carbon possessed high mesostructural ordering and SO_3H density (1.70–1.95 mmol/g), showing high performance for phenol condensation with acetone and oleic acid esterification with ethanol [194,195]. In a similar way, active carbon was functionalized with arene- SO_3H (0.64 mmol/g), but one third of the acid sites were leached after usage in the esterification reaction of acetic acid with ethanol [192]. Zhu and co-workers achieved the grafting of aryl SO_3H to γ - Al_2O_3 templated mesoporous carbon (from sucrose pyrolyzed at 600 °C [191] or resorcinol-furfural pyrolyzed at 500–1000 °C [190]) by using 4-benzene-diazoniumsulfonate without H_3PO_2 . The obtained sulfonated mesoporous carbon contains up to 1.72 [191] or 1.86 [190] mmol/g SO_3H , and was successfully applied for oleic acid esterification with methanol [190,191]. It was found that the weak acid groups such as OH and COOH, which existed in the incompletely carbonized organics, occupied edge positions of the carbon sheets that would otherwise be attached to arene- SO_3H , and hence led to a decrease in SO_3H density for samples pyrolyzed at a low temperature [190]. Malins and co-workers raised the arylation temperature to 70 °C without using H_3PO_2 , and active carbon with higher SO_3H groups (0.72 mmol/g) was obtained for the free fatty acids esterification [196].

4-Benzene-diazoniumsulfonate can also be *in situ* generated by isooamyl nitrite and 4-aminobenzenesulfonic acid at 30 °C to introduce sulfophenyl groups on the surface of mesoporous carbon, hollow mesoporous carbon spheres and carbon nanofibers [193,197–199]. Guo and co-workers carried out this diazium coupling reaction with hollow carbon spheres obtained from hard-templating synthesis with silica core/mesoporous aluminosilicate shell structure and furfuryl alcohol followed by pyrolysis at 600 °C [193]. The resultant ArSO_3H functionalized mesoporous carbon shells had a high porosity and 0.86 mmol/g SO_3H , showing a high catalytic activity for furfuryl alcohol ethanolysis and levulinic acid esterification reactions [193]. Tang and co-workers found that the pyrolysis temperature of mesoporous carbon from EISA of resol/F127 should be low enough to ensure more active sites for the grafting of benzenesulfonic radical; 2.28 and 0.83 mmol/g SO_3H for 400 and 800 °C pyrolyzed sample respectively were achieved [197]. This conclusion is in contrast with that of Zhu and co-workers [190]. It is therefore speculated that not only the amount of oxygen-containing groups and the size of carbon sheets that influence the sulfonation efficiency, but also the porosity which is closely related to the pyrolysis temperature, influences the radical arylation reaction. Although the grafting of arene- SO_3H using diazium salt creates covalent attachment and maintains the mesoporous channels, this method significantly decreases the surface area and pore volume of the material, and there are many side reactions as a result of the highly reactive radicals.

3.2.4. SH or SO_3H terminated organosilanes

SH or SO_3H terminated organosilanes are also a type of organosulfonic acid precursors. Grafting such organosilanes using cross-linking reactions with surface silanol groups is one of the most important approaches to make SO_3H functionalized mesoporous organosilica hybrids [22–25,200]. MPTMS is frequently applied, for example,

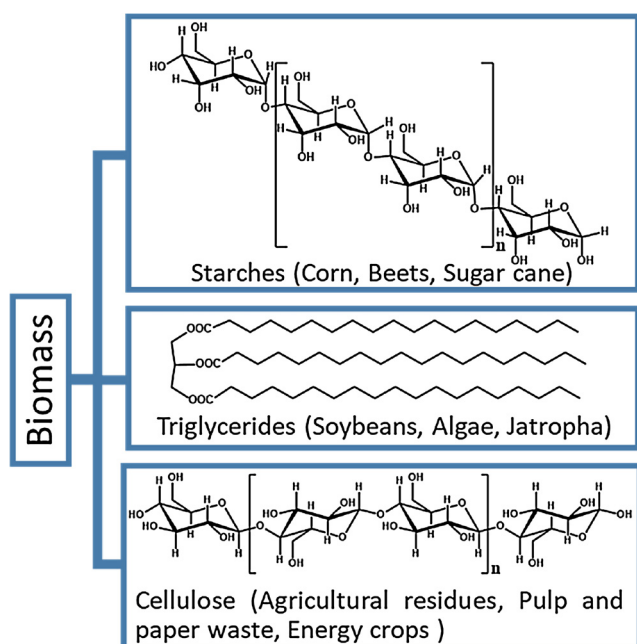


Fig. 9. Chemical structures of biomass feedstocks: starches, triglycerides and cellulose (the predominant component of lignocellulosic biomass). Reproduced with permission from Ref. [206]. Copyright 2010 Royal Society of Chemistry.

to be anchored in the mesopores of calcined MCM-41 (0.4 mmol/g SO₃H) [201] and SBA-15 (0.8 mmol/g SO₃H) [162], via a subsequent oxidation with H₂O₂. However, due to the less stable anchoring, uneven distribution and decreased porosity caused by post-synthetic grafting, co-condensation is often preferred to synthesize similar mesoporous organosilicas [25]. The merits of grafting organosilanes lie in the viability to modify surfaces as long as the silylation reaction occurs. Van Der Voort and co-workers used MPTMS and 2-(4-chlorosulfonylphenyl) ethyl trichlorosilane to modify the mesoporous phenolic resin from macroscopic phase separation synthesis of resorcinol-formaldehyde/F127 [202]. The thiol-containing silane and chlorosulfonyl-containing silane afford the sulfonated mesoporous carbons with 0.74 and 0.52 mmol/g SO₃H respectively, which still have high surface areas for the asymmetric aldol reaction of 2-butanone with 4-(trifluoromethyl) benzaldehyde [202].

4. Application in biomass conversion

The development of sustainable and green energy is of great importance due to energy crisis and environmental pollution in the current society. Biomass has received considerable attention as a renewable and sustainable feedstock for the production of bioenergy, biofuels and bio-based chemicals, which show potential to at least partially replace and complement current non-renewable fossil resources [203–210]. There are three important classes of biomass feedstock: starches, triglycerides and lignocellulosic biomass, as shown in Fig. 9 [206]. Starchy feedstock is easy to process while competing against food supply unless waste streams are used. Triglyceride feedstock consists of fatty acids and glycerol derived from both plant and animal sources. Lignocellulosic biomass is most abundant and non-edible biomass, such as woody biomass and agricultural residues. Hence, the catalytic conversion of triglycerides and lignocellulosic biomass to fuels and platform chemicals has been intensively studied, among which many reactions are catalyzed by strong Brønsted acids [207–212]. Fundamental challenges in catalyst design lie in the accessibility, activity and stability of these acid sites. Sulfonated mesoporous carbon or silica-carbon nanocomposites, featured by a high density of strong SO₃H acidic groups, well-ordered mesoporous structure, specific

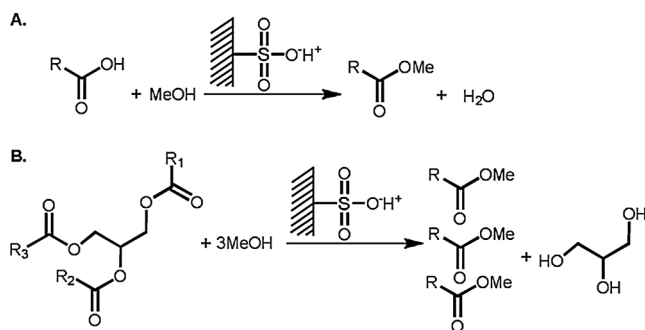


Fig. 10. (A) Esterification of fatty acids and (B) transesterification of triglycerides.

affinity of the surface and high hydrothermal stability, are thus promising for such biomass conversions in liquid phase.

4.1. Transformation of triglyceride feedstock

The triglyceride feedstock, such as crude vegetable oil, can be transformed through esterification of fatty acids or transesterification of triglycerides with alcohols by a solid acid catalyst (Fig. 10) [148,213]. The obtained fatty acid esters are the first generation biodiesel, a clean-burning alternative fuel [148,206,213]. Meanwhile, fatty esters are important emulsifiers, surfactants, lubricants and low calorie substitutes of edible fat [148].

4.1.1. Esterification of fatty acids

As a heterogeneous counterpart of H₂SO₄, SO₃H functionalized amorphous carbon [125,128,141,153,156,170,172,174,214–216], mesoporous carbon [49,94,176,190,191,194,196,197,217] and mesoporous silica-carbon nanocomposites [38,39,218] have been reported to be efficient catalysts for the esterification reaction of fatty acids, such as oleic acid, palmitic acid and stearic acid with methanol or ethanol. Table 2 summarizes the main results reported in the esterification reactions of fatty acids using sulfonated carbon or silica-carbon nanocomposites catalysts.

The sulfonated amorphous carbon consists of aggregates of polycyclic aromatic carbon sheets bearing phenolic OH, COOH and SO₃H, but it lacks a high surface area. These materials can incorporate large amounts of hydrophilic molecules into the carbon bulk by diffusion and swell to provide the accessibility, thus showing catalytic activity [122,125]. However, this improvement of accessibility will be largely impaired with the highly cross-linked carbon sheets from higher pyrolysis temperature, resulting in a rather poor catalytic activity despite the significant amounts of SO₃H groups [122,123]. In the sulfonated mesoporous carbon or silica-carbon nanocomposites, high surface areas and large mesopores favour the mass transfer of large organic molecules, particularly enhancing the average catalytic turnover frequency (TOF, h⁻¹) at the acid site [190]. The other co-existing functional groups, for example, the weak acid sites like phenolic OH and COOH functionalities can play a cooperative role with SO₃H [214]. Hydrophobic domains, such as dodecylbenzene, can be introduced to the carbonaceous surface as well, to enrich the local concentration of substrate molecules and dispel reaction generated H₂O [153].

Regarding the stability of SO₃H-containing carbons in the esterification reactions, some literature has reported deactivation, while others observed the opposite, as shown in Table 2. The underlying reason could be that some deactivation processes are altered by comparing runs at different reaction times [219]. The hydrothermal stability of C–S O₃H linkages of the model sulfonic acid compounds follows the order of substituted aromatics < non-substituted aromatics < alkanes [220]. Nevertheless, the esterification reaction temperature is much lower than the temperatures for desulfonation; for instance, benzene sulfonic acid degrades in H₂O at 160 °C [220]. The

Table 2
Sulfonated carbon and silica-carbon nanocomposites used in the esterification of fatty acids, with short chain alcohols.

Catalyst	Preparation procedure	S_{BET} (m ² /g)	^a (mmol/g)	Reaction conditions ^b	Yield of ester ^c (%)	Stability	Ref.
Carbon(concentrated H ₂ SO ₄)	Glucose pyrolyzed at 400 °C and sulfonated in concentrated H ₂ SO ₄	2	0.7	Oleic acid + EtOH. MR = 10, t = 1 h, T = 80 °C, Cat = 7 wt%	26.4	Not reported	[125,156,170]
Carbon(fuming H ₂ SO ₄)	Glucose pyrolyzed at 400 °C and sulfonated in fuming H ₂ SO ₄	1	1.2	Oleic acid + MeOH. MR = 26, t = 1 h, T = 95 °C, Cat = 17 wt%	51.6	Stable	[122]
CCSA-400	Cellulose pyrolyzed at 400 °C and sulfonated in fuming H ₂ SO ₄	< 5	1.8	Oleic acid + MeOH. MR = 10, t = 6 h, T = 80 °C, Cat = 5 wt%	62.0	Stable	[128]
Ca-648,0,5-Sul-423 K15	Bagasse pyrolyzed at 375 °C and sulfonated in concentrated H ₂ SO ₄	< 5	1.06	Oleic acid + MeOH. MR = 10, t = 12 h, T = 80 °C, Cat = 5 wt%	95.0	Stable	[216]
Glu-Corn75	Mixture of glucose and starch pyrolyzed at 400 °C and sulfonated in concentrated H ₂ SO ₄	< 5	Not reported	Oleic acid + MeOH. MR = 10, t = 12 h, T = 80 °C, Cat = 5 wt%	96.8	Deactivated by leaching, but regenerated with concentrated H ₂ SO ₄ to 90% yield	[215]
P-C-SO ₃ H	Glucose impregnated in polymer matrix pyrolyzed at 300 °C and sulfonated in concentrated H ₂ SO ₄	< 1	2.42	Palmitic acid + MeOH. MR = 6, t = 1 h, T = 60 °C, Cat = 2 wt%	21.3	Stable	[215]
C-SO ₃ H	Glucose pyrolyzed at 400 °C and sulfonated in concentrated H ₂ SO ₄	< 1	0.66	Palmitic acid + MeOH. MR = 33, t = 5 h, T = 64 °C, Cat = 100 wt %	12.7	Deactivated by leaching	[177]
SO ₃ H-SWCNHS	Single-walled carbon nanohorns, sulfonated in concentrated H ₂ SO ₄	418	0.50	Stearic acid + MeOH. MR = 15, t = 15 h, t = 1 h, T = 60 °C, Cat = 14 wt%	93	Deactivated by reducing the number of acid sites during the first run, but not observed for the next 2 runs	[177]
PHC-400C-SO ₄	Pelletized peanut hull char pyrolyzed at 400 °C and sulfonated in concentrated H ₂ SO ₄	242	0.61	Palm fatty acid distilled + MeOH. MR = 10, t = 2 h, T = 75 °C, Cat = 2.5 wt%	90.0	Continuously deactivated after MeOH washing, but partly regenerated by heptane rinsing	[172]
ICG _{0.15} -SO ₃ H	Glucose pyrolyzed at 400 °C and sulfonated in concentrated H ₂ SO ₄	11	1.53	Oleic acid + MeOH. MR = 68, t = 10 h, T = 65 °C, Cat = 9.8 wt %	92.3	Gradually deactivated by leaching	[174]
Carbon based solid acid catalyst	Glycerol hydrothermally sulfonated and carbonized in concentrated H ₂ SO ₄ at 180 °C	87	1.03	Palmitic acid + MeOH. MR = 10, t = 2 h, T = 75 °C, Cat = 5.2 wt %	95 (Conv.)	Stable	[158]
HC-SO ₃ H	Glucose hydrothermally carbonized at 190 °C and sulfonated in concentrated H ₂ SO ₄	7	0.55	Oleic acid + MeOH. MR = 5, t = 4 h, T = 65 °C, Cat = 8.9 wt %	46	Deactivated mainly by the formation of sulfonate esters	[141,214]
F-S	Furfural-sodium dodecylbenzene sulfonate-H ₂ SO ₄ hydrothermally carbonized at 180 °C	40	1.1	Palmitic acid + MeOH. MR = 10, t = 1 h, T = 85 °C, Cat = 7.1 wt %	59	Not reported	[153]
CMK-3-87-3-SO ₃ H	Hard-template synthesis with SBA-15 and sucrose, pyrolyzed at 600 °C, sulfonated in concentrated H ₂ SO ₄ and removal of SiO ₂	807.8	0.39	Oleic acid + MeOH. MR = 56, t = 6 h, T = 80 °C, Cat = 2 wt%	70 (Conv.)	Decrease to 51% after 4 runs, not due to leaching, but due to loss of powder or accumulation of impurities	[176]
SC-Al-900	Hard-template synthesis with γ -Al ₂ O ₃ and resorcinol-furfural, pyrolyzed at 900 °C, removal of Al ₂ O ₃ and sulfonated using diazoniumsulfonate	1118	1.86	Oleic acid + MeOH. MR = 56, t = 1 h, T = 65 °C, Cat = 2 wt%	59	Regenerated by 0.1 M H ₂ SO ₄ but still deactivated due to the loss of acid sites (1.34 mmol/g after 6 runs)	[190]
C-CCA1	Hard-template synthesis with γ -Al ₂ O ₃ and sucrose, pyrolyzed at 600 °C, removal of Al ₂ O ₃ and sulfonated using diazoniumsulfonate	570	1.72	Oleic acid + MeOH. MR = 56, t = 0.5 h, T = 65 °C, Cat = 5 wt %	61.3	Not reported	[191]
CMK-w-SO ₃ H	Sucrose was added to TEOS in the presence of HCl and H ₃ PO ₄ , pyrolyzed at 400 °C, removal of SiO ₂ and sulfonated in fuming H ₂ SO ₄	< 1	1.1	Oleic acid + MeOH. MR = 10, t = 4 h, T = 80 °C, Cat = 7 wt%	78	Not reported	[37]
CMK-SO ₃ H-w	Sucrose was added to TEOS in the presence of HCl and H ₃ PO ₄ , pyrolyzed at 400 °C, sulfonated in fuming H ₂ SO ₄ and removal of SiO ₂	588	0.7	Oleic acid + MeOH. MR = 3, t = 1 h, T = 60 °C, Cat = 2.9 wt %	29	Not reported	[217]
CMH-200-1273-SO ₃ H	Resorcinol-formaldehyde resin aerogel pyrolyzed at 1000 °C and sulfonated in concentrated H ₂ SO ₄	570	0.62	Oleic acid + MeOH. MR = 20, t = 2 h, T = 70 °C, Cat = 0.7 wt %	53 (Conv.)	Stable	[49]
OMC-H ₂ O ₂ -SO ₃ H	Hard-template synthesis with SBA-15 and furfuryl alcohol, pyrolyzed at 800 °C, removal of SiO ₂ , oxidized by H ₂ O ₂ and sulfonated in concentrated H ₂ SO ₄	475	1.86	Oleic acid + MeOH. MR = 20, t = 2 h, T = 70 °C, Cat = 0.7 wt %	86 (Conv.)	Stable	[49]

(continued on next page)

Table 2 (continued)

Catalyst	Preparation procedure	S_{BET} (m ² /g)	^a (mmol/g)	Reaction conditions ^b	Yield of ester ^c (%)	Stability	Ref.
MC-4-SO ₃ H	Soft-template synthesis of F127/resorcinol-formaldehyde, pyrolyzed at 400 °C and sulfonated in concentrated H ₂ SO ₄	120	1.87	Oleic acid + MeOH, MR = 30, t = 3 h, T = 70 °C, Cat = 0.7 wt %	75 (Conv.)	Stable	[94]
S-OMC-500	Soft-template synthesis of F127/phenol-formaldehyde, pyrolyzed at 500 °C and sulfonated using diazoniumsulfonate	594	2.16	Oleic acid + MeOH, MR = 10, t = 6 h, T = 120 °C, Cat = 10 wt %	96.3 (Conv.)	Stable	[197]
ACPhSO ₃ H	Activated carbon sulfonated using diazoniumsulfonate	114	0.72	Rapeseed oil fatty acids acid + MeOH, MR = 20, t = 2 h, T = 65 °C, Cat = 10 wt %	65 (Conv.)	Deactivated due to leaching of PhSO ₃ H groups but regenerated by redoing the arylation reaction	[196]
OMC-SO ₃ H-150	Hard template synthesis with SBA-15 and furfuryl alcohol, pyrolyzed at 850 °C, removal of SiO ₂ and sulfonated using diazoniumsulfonate	741	1.70	Oleic acid + EtOH, MR = 10, t = 10 h, T = 80 °C, Cat = 3.5 wt %	73.6 (Conv.)	Stable	[194]
SBA-15-ph-SO ₃ H	Synthesized by co-condensation of CSPTMS and TEOS, removal of P123 and oxidized with H ₂ O ₂	610	1.17		51.0 (Conv.)	Deactivated due to the hydrolysis of Si-O-Si-R siloxane bonds	
Silica functionalized with 4-ethyl-1-benzene sulfonic groups	Commercial	317	0.94	Sunflower oil + MeOH, MR = 6, t = 5 h, T = 150 °C, Cat = 1.5 wt %	60	Severely deactivated due to leaching of organosulfonic groups and deposition of organic species	[218]
25%C/CS-SO ₃ H	Hard-template synthesis with SBA-15 and sucrose, pyrolyzed at 400 °C and sulfonated using vapor of fuming H ₂ SO ₄	358	0.44	Palmitic acid + MeOH, MR = 30, t = 2 h, T = 70 °C, Cat = 5 wt %	88	Not reported	[39]
CSK-500	Hard-template synthesis with KIT-6 and 2,3-dihydroxynaphthalene, pyrolyzed at 500 °C and sulfonated in concentrated H ₂ SO ₄	590	0.38	Palmitic acid + EtOH, MR = 10, t = 1 h, T = 78 °C, Cat = 2.8 wt %	8	Stable	[38]
OSMCF-1,100-SO ₃ H	Co-condensation synthesis of 1,4-bis(triethoxysilyl)-benzene and TEOS in the presence of P123 and 1,3,5-trimethylbenzene, washed by HCl and EtOH, and sulfonated in concentrated H ₂ SO ₄ , K ₂ S ₂ O ₈	597	0.95	Oleic acid + MeOH, MR = 30, t = 6 h, T = 100 °C, Cat = 50 wt %	89.7 (Conv.)	Not reported	[181]
CX4SO ₃ H-SiO ₂	<i>p</i> -Sulfonic acid calix[4]arene was added to TEOS in the presence of HCl		Not reported	Palmitic acid + EtOH, MR = 439, t = 4 h, T = 80 °C, Cat = 100 wt %	88	Stable	[168]

^a Represents the SO₃H group density in the catalyst.^b MR is the molar ratio of methanol or ethanol to fatty acid. *t* is the reaction time. *T* is the reaction temperature. Cat is the catalyst loading with respect to the fatty acid.^c (Conv.) denotes that the conversion of fatty acid is provided instead of the yield of fatty ester.

deactivation therefore mainly roots in the leaching of sulfonated aromatic fragments of the catalyst and the deposition of organics (*i.e.* irreversible adsorption) that foul and block the active sites. Leaching of sulfonated polycyclic aromatic hydrocarbon is due to the solubility of the compounds in solvents like methanol, ethanol, H_2O , hexane, *etc.* [171]. Meanwhile, such loss of active sites highly depends on the type of reaction substrates. Hara and co-workers reported a solid catalyst from a one-step sulfonation and carbonization of naphthalene in concentrated H_2SO_4 , which was recyclable for esterification of acetic acid with ethanol [155]. However, the catalyst deactivates in the esterification of oleic acid, since oleic acid likely acts as a surfactant that increases the solubility of the sulfonated aromatic carbon [156]. The leaching problem can be solved by increasing the interaction of organosulfonic acid with the catalyst framework. Goodwin and co-workers carried out the pyrolysis of glucose within a polymeric resin matrix, and after sulfonation, the catalyst showed much higher stability than the material from pyrolysis of only glucose [215]. Valente and co-workers also found that the silica-carbon nanocomposites with SO_3H groups from the pyrolysis of SBA-15 infilled with TsOH was not stable for HMF ethanolysis [45]. H_2SO_4 which can catalyze the cross-linking of aromatic compounds, was therefore added to increase the carbonization degree and achieve a stable solid acid catalyst [45]. Sulfonated catalysts that are functionalized post-synthetically can also be recovered by simply redo the sulfonation procedure as long as the pore structure is more or less maintained [196,216]. On the other hand, the deposition of organics seem more difficult to tackle as the commonly adopted calcination procedure (under oxygen or hydrogen) will destroy the carbon-based catalyst. The deposited organics may change the nature of active sites such as forming sulfonate esters [141,214], or they foul and block the active sites for the heavy components, such as reducing the surface area and pore size [172,218]. Washing by heptane can only partly recover the catalyst activity of sulfonated biochar for the esterification of soybean oil [172]. Therefore, it is better to find alternative oxidants that can remove the organics selectively without destroying the C–S O_3H sites and the pore structure too much. In fact, concentrated H_2SO_4 is a promising agent under this circumstance. The sulfonation by concentrated H_2SO_4 of a spent catalyst (Glu-Corn75) can thus be almost completely restored for the esterification reaction of oleic acid with methanol [216]. However, the surface chemistry and mechanism, as well as the broad applicability of this recovery methodology require further investigation.

4.1.2. Transesterification of triglycerides

Glycerol in triglycerides can be exchanged with other alcohols such as methanol and ethanol through the hydrolysis of triglycerides-esterification of fatty acids, resulting in fatty esters such as methyl oleate, palmitate and linolate [148,213]. While such reaction is usually catalyzed with base, many sulfonated carbon or silica-carbon nanocomposites catalysts have been examined for the transesterification reaction, at a temperature higher than the esterification reaction [117,122,158,171,198]. Sulfonated amorphous carbon from the pyrolysis of cellulose and subsequent sulfonation in fuming H_2SO_4 showed stable catalytic performance for transesterification of triolein (51% yield of methyl oleate after 2 h at 130 °C for 6 runs) [122]. Similarly, sulfonated polycyclic aromatic sheets bearing SO_3H , phenolic OH and COOH groups from concurrent sulfonation and carbonization of glycerol in concentrated H_2SO_4 , showed a high yield of methyl oleate from transesterification [158]. The affinity of the flexible carbon sheets to incorporate the solvent molecules (*i.e.* by swelling) is supposed to improve the diffusion [122,158,171]. However, the swelling also affects the dissolution of sulfonated polycyclic aromatic hydrocarbons causing leaching of acids [171,198]. Bitter and co-worker developed carbon nanofibers sulfonated with diazoniumsulfonate as a highly active catalyst for transesterification of triolein with methanol [198]. They demonstrated that aryl- SO_3H functionalized carbon nanofiber was equally active compared to the sulfonated cellulose-derived carbon, but much

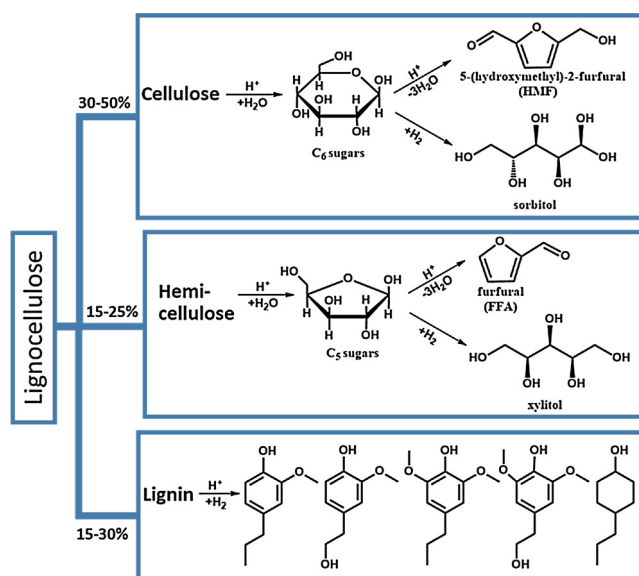


Fig. 11. Targeted chemical upgrading of lignocellulosic biomass. Reproduced with permission from Ref. [205]. Copyright 2014 Royal Society of Chemistry.

more stable for recycling [198]. Yang and co-workers synthesized sulfonated polystyrene-silica composite hollow nanospheres for the transesterification of tripalmitin with methanol [117]. Due to the open mesoporous shell structure, SO_3H groups can be easily accessed and high yield of methyl palmitate was obtained [117]. The surface modification by octyl and perfluorinated octyl groups can increase the hydrophobicity for the surface, lead to pore enrichment of hydrophobic tripalmitin and prevent the leaching of polystyrene- SO_3H , thus resulting in an even more active and stable solid acid catalyst [117].

4.2. Transformation of lignocellulosic biomass

Lignocellulose, the most abundant renewable biomass feedstock, consists mainly of cellulose, hemicellulose and lignin, as shown in Fig. 11. Many attempts have been made to develop heterogeneous catalytic processes for the conversion of non-food lignocellulose, with the aim of finding potential industrial applications. Sulfonated carbon or silica-carbon nanocomposites as an important class of H_2O -tolerant strong Brønsted acid solid catalysts, have been widely applied for the liquid-phase up-grading of lignocellulose to biofuels and bio-based chemicals, including the hydrolysis of cellulose and hemicellulose to monomers and their conversion mainly via a furan platform (Fig. 12). Many biomass transformation reactions belong to the one-pot cascade type of reactions employing multifunctional catalysis. For example, Sels and co-workers prepared Sn grafted MCM-41-templated silica-carbon nanocomposites which contained both Lewis and Brønsted acid sites to achieve one-pot conversion of dihydroxyacetone to lactate [48]. However, the application of SO_3H sites in combination with other types of catalytic functionalities is outside the scope of this review. The use of C–S O_3H containing solid acids is the focus of this contribution.

Carbohydrates, like hexoses (C₆-sugars) and pentoses (C₅-sugars) are the units of polysaccharides in many biomass resources such as cellulose, hemicellulose, starch, glycogen and inulin. Hydrolysis in the presence of SO_3H acids produces C₆ and C₅ sugars such as glucose, fructose and xylose [205,209]. Besides the hydrolysis reactions, the strong Brønsted acid sites can facilitate the consecutive catalytic dehydration of monosaccharides to yield platform chemicals like HMF (from fructose) and furfural (from xylose) [203]. As shown in Fig. 12, based on HMF and furfural, many other reactions, such as rehydration, esterification and condensation may occur under the action of SO_3H catalysis as well. For the optimization of the yield of targeted products,

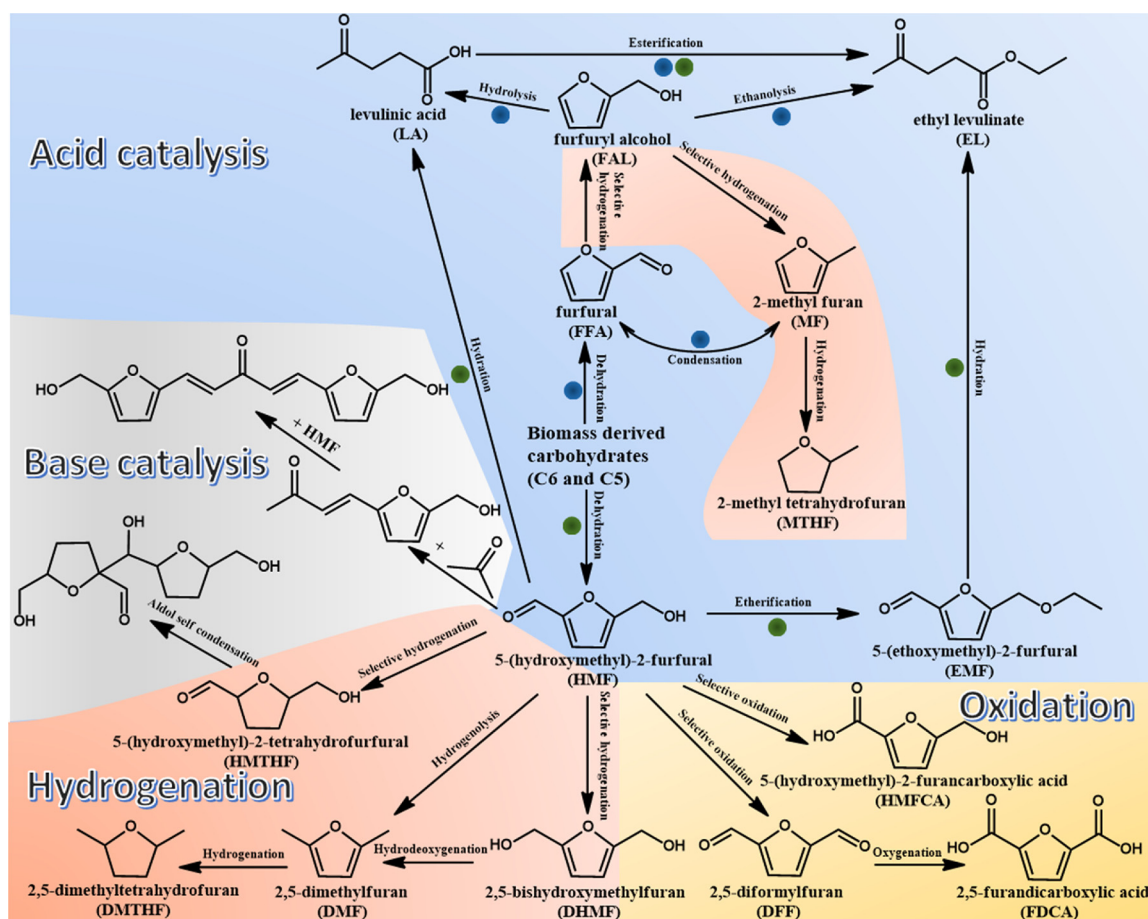


Fig. 12. Furan platform of carbohydrates conversion. The green and blue dots represent the catalysis by Brønsted acid for HMF-mediated and furfural-mediated pathways, respectively (For interpretation of the references to colour in this figure legend, the reader is referred to the web version of this article).

minimizing the formation of polymeric humins is one of the key challenges. Humins are formed in a similar way to the reactions in a hydrothermal carbonization process, *via* the oligomerization and polymerization of reactive furanic intermediates [136,221]. There are soluble and insoluble humins, both adverse for the production of the desired chemicals [221].

4.2.1. Hydrolysis of cellulose or hemicellulose to monosaccharides

Cellulose is the most abundant natural biopolymer composed of glucose units linked by β -1,4 glycosidic bonds. Intra- and intermolecular hydrogen bonds in the cellulose network makes the structure very recalcitrant for the hydrolysis [209,222,223]. Cellulose is therefore often treated by ball-milling to decrease the crystallinity though other unconventional pretreatments are used as well [68,140,161,181,224,225]. Use of short β -1,4 glucan like cellobiose instead as a substrate for the study of cleavage of β -1,4 glycosidic bonds is another option to avoid the recalcitrance [124,129]. Glucose from hydrolysis of cellulose is a versatile precursor to important chemicals such as ethanol, HMF, glucoside, hexitol, ethylene glycol and gluconic acid [222,226].

Table 3 presents recent results of hydrolysis of cellulose obtained with sulfonated carbon or silica-carbon nanocomposites catalysts. Sulfonated amorphous carbons derived from the pyrolysis of cellulose or glucose and sulfonation in fuming H_2SO_4 were applied for the hydrolysis of cellobiose [124,129]. The phenolic OH and COOH groups in the incompletely carbonized carbohydrates adsorb β -1,4 glucan and H_2O molecules effectively through H-bonding, facilitating the catalytic hydrolysis of glycosidic bonds by SO_3H groups [124,129]. The apparent activation energy is 110 kJ mol^{-1} , significantly lower than that of

H_2SO_4 (170 kJ mol^{-1}) [129]. The hydrothermally formed carbonaceous materials after sulfonation are also active for the hydrolysis of ball-milled cellulose [140,225]. The yield of glucose reaches 74%, which is higher than the value in the presence of the carbon-based sulfonated catalyst derived from the pyrolysis procedure [140]. During the recycling experiments, there are slight losses of SO_3H groups and cellulose conversions slightly drop [225]. The spent carbonaceous solid acid can be regenerated by treatment in 40% H_2SO_4 solution at 100°C , which leads to a recovery of glucose yield to 50% compared to 57% for the fresh catalyst [139]. Another way of regeneration is through redoing the pyrolysis and sulfonation, which restores the glucose yield for the second run, 31.3% in comparison with 32.7% for the fresh catalyst [227]. Zhang and co-workers tested sulfonated mesoporous carbons from hard-template (CMK-3- SO_3H) and soft-template (Resin-Carbon- SO_3H) syntheses for the hydrolysis of ball-milled cellulose [161]. They both gave higher glucose yields than that of amorphous carbons - the highest yield 74.5% was obtained with CMK-3- SO_3H - due to the large surface area and mesoporous structure, which facilitate the transportation of substrates and allow facile access to SO_3H groups [161]. Sulfonated silica-carbon nanocomposites from the EISA synthesis of sucrose/TEOS/F127 were also applied for cellulose hydrolysis, providing a high yield of glucose 50.4% and staying stable for 3 recycles after slight initial loss of sulfonated polycyclic aromatic carbon [68]. The sulfonated benzene-bridged organosilica mesocellular foam showed a high 75.6% glucose yield from microcrystalline cellulose, at a low temperature of 100°C for a short time of 1 h [181]. Besides the large pores and high SO_3H density (0.95 mmol/g) of the catalyst, the co-solvent ionic liquid, 1-butyl-3-methyl imidazolium chloride ([BMIM] $[\text{Cl}]$) plays an important role in increasing the solubility of cellulose

Table 3
The catalytic reaction results for the hydrolysis of cellulose with sulfonated carbon or silica-carbon nanocomposites.

Catalyst	Preparation procedure	S_{BET} (m ² /g)	^a (mmol/g)	Substrates ^b	T (°C)	t (h)	Cat. ^c (wt%)	Yield ^d (%)	Stability	Ref.
carbon material ($\text{CH}_{0.2} \text{O}_{0.54} \text{S}_{0.05}$)	Cellulose pyrolyzed at 450 °C, and sulfonated in fuming H_2SO_4	< 5	1.9	Crystalline cellulose	100	3	1200	4	Stable	[129]
CCSA-673	Cellulose pyrolyzed at 400 °C, and sulfonated in fuming H_2SO_4	< 5	1.8	Cellulose	100	6	100	35	Stable	[124]
CSA	Glucose hydrothermally treated at 180 °C, and sulfonated in fuming H_2SO_4	Not reported	1.86	Ball-milled cellulose	150	0.67	1000	74.0 ^e	Not reported	[140]
Sulfonated sucrose carbon	Sucrose hydrothermally treated at 180 °C, and sulfonated in concentrated H_2SO_4	Not reported	0.225	Crystalline cellulose	120	4	100	59 ^f	Deactivated due to leaching of SO_3H groups and ion-exchange reactions, but regenerated by treatment in 40% H_2SO_4 solution at 100 °C	[139]
$\text{Fe}_3\text{O}_4@\text{C-SO}_3\text{H}$	Glucose hydrothermally treated in the presence of FeCl_3 and urea at 180 °C, and sulfonated in concentrated H_2SO_4	Not reported	1.30 ^g	Ball-milled cellulose	140	12	300	25.3	Slightly deactivated due to leaching of SO_3H	[225]
GMK-3-SO ₃ H-250	Hard template synthesis with SBA-15 and sucrose, pyrolyzed at 900 °C, removal of SiO_2 , and sulfonated in concentrated H_2SO_4	41.2	0.63	Ball-milled cellulose	150	24	111	74.5	Stable	[161]
OSMCF-1,100-SO ₃ H	Co-condensation synthesis of 1,4-bis(trimethoxysilyl)-benzene and TEOS in the presence of P123 and 1,3,5-trimethylbenzene, washed by HCl and EtOH, and sulfonated in concentrated H_2SO_4 - $\text{K}_2\text{S}_2\text{O}_8$	597	0.95	Crystalline cellulose	100	1	30	75.6 ^f	Not reported	[181]
SI33C66-823-SO3H	Soft template synthesis of Sucrose/TEOS/F127, pyrolyzed at 550 °C, and sulfonated in concentrated H_2SO_4	0	0.37	Ball-milled cellulose	150	24	100	50	Decrease to 44% after the first run, due to leaching of some polycyclic aromatic hydrocarbon-containing SO_3H groups, but stable for the next 3 runs	[68]

^a Represents the SO_3H group density in the catalyst.

^b The substrate used in the hydrolysis reaction.

^c The solid acid catalyst weight ratio in relative to the substrate weight.

^d The yield of glucose = (mol of glucose produced by the hydrolysis)/(total mol of glucose monomer in the substrate) \times 100%.

^e The reaction mixture was heated in a microwave reactor.

^f The reaction solvent was [BMIM][Cl] with the presence of H_2O below 5 wt%.

^g The value includes the density of weak acid sites.

[139,223].

The solvolysis of cellulose in the presence of SO_3H acid sites can be carried out in an alcoholic solution. Riisager and co-workers performed the ethanolysis of cellobiose, using SO_3H -SBA-15 synthesized from co-condensation of MPTMS and TEOS followed by washing and H_2O_2 oxidation [162]. The formed glucose is subsequently converted into ethyl glucosides *via* acetalization (glycosylation) reactions. The final product is ethyl glucosides, the same as the product of the reaction starting from glucose [162]. The SO_3H Brønsted acid sites alone were not efficient for catalyzing the isomerization step of glucose to fructose which involves a hydride transfer [203]. Indeed, under the applied reaction conditions, fructose should undergo further reactions to 5-ethoxymethylfurfural (EMF) and ethyl levulinate (EL), but these products were not observed.

Hemicellulose such as xylan is composed of different C_5 and C_6 sugar units, with xylose being the most abundant monomer [205,212]. A combined yield of xylose and arabinose of *ca.* 50%, was obtained from the hydrolysis of xylan, using sulfonated silica gel synthesized by grafting of MPTMS onto silica surface and H_2O_2 oxidation [228]. After loss of loosely bound SO_3H groups during the first run, the recycled catalyst showed stable yield of *ca.* 25% in the next 3 runs [228]. The relatively low catalytic performance of SO_3H acid sites for hemicellulose hydrolysis is probably due to the subsequent degradation of C_5 -sugars, which will be discussed in 4.2.3, and the large amount of formed humins accompanies with it.

4.2.2. Dehydration of fructose to HMF and opening of the furanic ring

Fructose can be dehydrated to HMF in the presence of a Brønsted acid catalyst [210,229,230]. The dehydration of the furanose form of fructose is thermodynamically favourable due to the development of a conjugated π -electron system in the furanic ring [230]. HMF is a versatile valuable platform molecule for the synthesis of promising chemical intermediates. As shown in Fig. 12, HMF can be oxidized to 2,5-furandicarboxylic acid (FDCA), which can serve as a replacement of petrochemistry-derived terephthalic acid for polyesters synthesis [229]. The hydrogenation product (2,5-dimethylfuran, DMF) and etherification product (5-ethoxymethylfurfural, EMF) of HMF are excellent miscible diesel biofuels, with high energy densities [229]. However, HMF is an unstable product and its furanic ring can be decomposed by Brønsted acid [203,230,231]. Therefore, to avoid unwanted by-product formation, it usually requires a continuous extraction to an organic solvent to reduce the contact time of acid-sensitive furan with the acid [203,212,229]. The application of the biphasic system, which commonly includes an acidic aqueous phase and an organic phase modifier, is an example of such extraction method [163,189,232]. The applied organic solvent can be methyl isobutylketone (MIBK), 2-butanol, tetrahydrofuran (THF), dimethylsulfoxide (DMSO), etc. [212]. Another way is to convert HMF with an appropriate solvent (such as a primary alcohol) to a more stable derivative - the etherified form of HMF, 5-alkoxymethylfurfural in this case [221]. The rehydration of HMF is found to follow a common mechanism for HMF rehydration, in which C-1 (aldehyde carbon) and C-6 (methylene carbon) of HMF are transformed to the carbon of formic acid and methyl carbon of levulinic acid (LA), respectively [231]. The hydration product, LA, is also a versatile platform molecule. It can be further converted to important fuels and chemical products such as levulinic esters, γ -valerolactone, 2-methyltetrahydrofuran (MTHF), 1,4-pentanediol, succinic acid, bisphenols and so on [233,234]. Table 4 summarizes a variety of catalytic studies on fructose-to-HMF dehydration (and subsequent furanic ring-opening reactions) using sulfonated carbon or silica-carbon nanocomposites under various reaction conditions, including different solvents, temperatures, times and catalyst loadings. Since different solvents basically determine the product distribution pattern of fructose dehydration and subsequent reactions, this list is presented according to the applied solvent type.

As shown in Table 4, the dehydration of fructose is mainly carried

out in organic, organic- H_2O co-solvent and ionic liquid solvent. The conversion of fructose in H_2O will lead to a massive amount of humins. For example, in the presence of CST-1, a sulfonated silica-carbon nanocomposite catalyst, only 20% of LA and 9% of HMF were obtained at a 95% fructose conversion [45]. In contrast, the sulfonated carbonaceous solid and sulfonated organosilica show remarkably high and stable HMF yield in a non-aqueous ionic liquid medium [144,235,236]. The ionic liquid was found to stabilize HMF in the reaction system, avoiding the further rehydration and reducing condensation to humins to a large extent [235,242]. The use of DMSO as solvent can offer an even higher yield of HMF (maximum 91%) from fructose in the presence of sulfonated amorphous carbon or arene- SO_3H functionalized ordered mesoporous carbon [152,237,238]. The mechanism lies in the modification of fructose tautomerization to more furanose forms and stabilization of C-1 aldehyde carbon of HMF for less rehydration and humins formation [237]. However, the separation of HMF from these polar organic solvents is very difficult, due to the high boiling point [207]. Therefore, as an alternative to the above high-boiling and expensive solvents, the readily available and low-boiling alcohols are applied as a medium for fructose dehydration reactions.

Take ethanol as an example, the commonly accepted reaction pathways include three consecutive reactions, fructose dehydration to HMF, HMF etherification to EMF and EMF rehydration to EL [40,45,162,185,240]. The reaction conditions can be tuned for optimization of the targeted products. A high yield of HMF can be obtained when the reaction time is short and the alcohol is with a longer alkyl chain such as 2-propanol and 2-butanol [53,182]. The adding of a certain amount of DMSO to the alcohol results in improved yields of the furan products and reduced yields of furanic ring-opening products [165,240]. The raise of reaction temperature will change the product distribution by increasing levulinic yield. Propyl- SO_3H functionalized mesoporous silica produced EMF as main product (63%) at 100 °C, while EL was the main product (56%) at 140 °C [162,239]. The catalyst loading relative to fructose is usually higher when levulinic is the targeted product [238]. In some cases, the combined yield of HMF-ether and levulinic ester is taken as a criterion instead, as they are both fine biofuels [40,45].

Nevertheless, the most important factor for fructose conversion and the selectivity to the desired product is both the acidic and structural properties of the catalyst used. Chen and co-workers compared the catalytic activity of CMK-5-BSA and Amberlyst-15 for fructose alcoholysis, which both have arene- SO_3H as active sites [238]. Amberlyst-15 showed higher yield for alkyl levulinate, due to its far more active sites, 4.9 *vs.* 1.84 mmol/g SO_3H in CMK-5-BSA [238]. Morales and co-workers applied both Ar- SO_3H -SBA-15 and Pr- SO_3H -SBA-15 for the conversion of fructose in ethanol-DMSO co-solvent [165]. Despite the similar silica mesostructure and acid concentration, Ar- SO_3H -SBA-15 exhibited a higher performance for the consecutive etherification step of HMF to EMF, attributed to the inherently stronger acid strength of arene- SO_3H than propyl- SO_3H [165]. Valente and co-workers carried out the fructose conversion in ethanol- H_2O co-solvent under the same reaction conditions with C/SBA(45) and CST-1, which were synthesized from the same carbon precursor and had similar SO_3H content and surface area [40,45]. C/SBA(45) showed significantly higher activity toward the formation of EMF and EL than fuming SiO_2 templated CST-1, probably owing to the large pore volume of C/SBA(45) [40,45]. The large pore-opening allows the accommodation of EMF and its further rehydration to EL [162]. Besides, surface hydrophilicity/hydrophobicity also influences the catalytic performance [53,182,241]. The high local surface hydrophobicity around SO_3H facilitates the dehydration of fructose to HMF [53,182], but retards the departure of HMF from the catalyst surface and the selectivity of HMF is lower than that in presence of the hydrophilic surface [241]. Thus, the surface hydrophobicity needs to be optimized for a preferable production of HMF from fructose. As for the stability of the catalyst, by investigation of fructose dehydration in flowing THF- H_2O (4:1), propyl- SO_3H modified

Table 4
The catalytic reaction results for fructose dehydration (and subsequent furanic ring-opening reactions) with sulfonated carbon or silica-carbon nanocomposites.

Catalyst	Preparation procedure	S_{BET} (m ² /g)	^a (mmol/g)	Reaction conditions			Yield ^d (%)	HMF	Levulinic ethers	Stability	Ref.
				Solvent ^b	T (°C)	t (h)					
CSS	Cellulose hydrothermally carbonized at 250 °C and sulfonated in concentrated H ₂ SO ₄	< 0.5	0.953	Cl	80	0.33	50	77	–	–	Deactivated to 72% after 4 runs [235]
D265-SO ₃ H	Xylose hydrothermally carbonized at 265 °C and sulfonated in concentrated H ₂ SO ₄	< 2	0.63	Cl ^e	100	1	100 (In.)	65 (In.)	–	–	Deactivated by loss of acid sites, but regenerated by 10% H ₂ SO ₄ [144]
SBA-15-SO ₃ H- 10	Co-condensation of TEOS and MPTMS, removal of P123	688.6	0.83	Cl	120	1	10	81	–	–	Deactivated to 73% after 3 runs [236]
Glu-TsOH	Glucose-TsOH hydrothermally carbonized at 180 °C and oxidized by H ₂ O ₂	< 1.0	1.3	DMSO	130	1.5	80	91.2	–	–	Stable [152]
CS-2	Glucose hydrothermally carbonized at 180 °C and sulfonated in H ₂ SO ₄ solution	40.17	0.17	DMSO	140	1	20	79	–	–	Deactivated to 71 after 4 runs [237]
CMK-5-BSA	Hard-template synthesis of SBA-15 and ionic liquid, pyrolyzed at 850 °C, removal of SiO ₂ and sulfonated using diazoniumsulfonate	Not reported	1.84	DMSO	120	0.5	10	76	–	–	Not reported [238]
GIOMC- Ar-SO ₃ H	Hard-template synthesis with SBA-15 and ionic liquid, pyrolyzed at 900 °C, removal of SiO ₂ and sulfonated using diazoniumsulfonate	665	0.7	Methanol	100	24	40	–	–	–	49
Fe ₃ O ₄ @C- SO ₃ H	Hard-template synthesis with Fe ₃ O ₄ microparticles and glucose under hydrothermal conditions at 200 °C, sulfonated using ClSO ₃ H	29.9	1.38	Ethanol	140	24	56 (In.)	2	67.8	18.7	Stable for reactions starting from HMF [185]
Silica-SO ₃ H	Co-condensation of TEOS and MPTMS in the presence of n-hexadecylamine, removal of surfactant and oxidized by H ₂ O ₂	1102	0.20	Ethanol	100	24	111	11.2	63.1	–	Slightly deactivated to 57.5% EMF yield after 5 runs [239]
SO ₃ H-SBA-15- D	Co-condensation of TEOS and MPTMS in the presence of P123, removal of surfactant and oxidized by H ₂ O ₂	819	0.73	Ethanol	140	24	30	< 1	11	56	Stably deactivated to 53% EMF yield after 2 runs [162]
SO ₃ H-SBA-15- PS	SBA-15 grafted with MPTMS and oxidized by H ₂ O ₂	589	0.81	Ethanol	140	24	30	< 1	12	57	Not reported [162]
GO	Graphite treated by Hummers method	Not reported	Not reported	Ethanol-DMSO (7:3)	130	24	33	9	71	–	Slightly deactivated to 64% EMF yield after 3 runs due to partial reduction of GO [240]
Ar-SO ₃ H-SBA- 15 C/SBA(45)	Co-condensation of TEOS and CSPTMS in the presence of P123, removal of P123 and oxidized by H ₂ O ₂	712	0.92	Ethanol-DMSO (11:1)	116	4	82	7 (In.)	66 (In.)	–	Not reported [165]
C/MCF(63)	Hard-template synthesis with SBA-15 and TsOH-H ₂ SO ₄ , pyrolyzed at 250 °C (MCF) and TsOH-H ₂ SO ₄ , pyrolyzed at 250 °C (MCF)	238	1.9	Ethanol-H ₂ O (7:3)	140	24	17	10	28	16	Slightly deactivated to 46 EMF yield after 3 runs due to deposition of humins [40]
CST-1	Hard-template synthesis with mesocellular silica foam (MCF) and TsOH-H ₂ SO ₄ , pyrolyzed at 250 °C (MCF) and TsOH-H ₂ SO ₄ , pyrolyzed at 250 °C (MCF)	198	2.3	Ethanol-H ₂ O (7:3)	140	24	17	6	24	21	Stable for reactions starting from HMF [40]
PMO-1a	Co-condensation of 1,4-(triethoxysilyl)benzene and MPTMS in the presence of ODTMA ^f , removal of surfactant and oxidized by HNO ₃	Not reported	1.11	MIBK/2-butanol(7:3) +H ₂ O	160	0.5	16	58	–	–	Deactivated after 2 runs [182]
SBA-15- PrSO ₃ H	Co-condensation of TEOS and MPTMS in the presence of P123, removal of surfactant and oxidized by H ₂ O ₂	682	1.2	Nitromethane-H ₂ O (9:1)	140	0.5	9	70	–	–	Deactivated due to the physical adsorption of by-produced humins [241]

^a Represents the SO₃H group density in the catalyst.

^b The ratio is the brackets is the volume ratio of the two solvents.

^c Cat. indicates the catalyst loading relative to fructose.

^d The brackets (In.) indicates inulin was used instead of fructose as substrate. Inulin is a natural polysaccharide consisting of mainly fructose units.

^e Cl is an ionic liquid, 1-allyl-3-methyl imidazolium chloride.

^f ODTMA is a surfactant, octadecyltrimethylammonium bromide.

SBA-15 is far less stable than the sulfonated mesoporous carbons from sulfonation by concentrated H_2SO_4 or diazoniumsulfonate [189]. The deactivation caused by Si-O-C bonds cleavage can be reduced by using propyl- SO_3H functionalized ethane-bridged SBA-15 type organosilica [163]. For the carbon-based SO_3H materials, the strong attachments *via* C–C and C–S bonds are less susceptible to hydrolysis, but the fouling of the active sites by humin degradation products is somewhat inevitable. Easy solutions to clean the active surface and re-activate the carbon catalyst are therefore challenging.

4.2.3. Dehydration of xylose to furfural and opening of the furanic ring

The dehydration ($-3H_2O$) of C₅ carbohydrate, xylose, produces furfural [229,243]. Furfural can undergo typical reactions of aldehyde to serve as a versatile chemical feedstock. Meanwhile, due to the electron-withdrawing effect of the carbonyl group, furfural is less susceptible to hydrolytic ring-opening [243]. Sulfonated ordered mesoporous organosilica hybrids [201,244,245], sulfonated pyrolyzed carbon derived from biomass [246], and silica-PSSA nanocomposites [169] have been used for the catalytic dehydration of xylose to furfural in various solvents, such as DMSO [201,246,247], 2-propanol [245] and toluene- H_2O [169,201,244,247]. Similarly to the situation of fructose dehydration to HMF in DMSO, xylose dehydration to furfural in DMSO also leads to high furfural yield. However, toluene- H_2O co-solvent appears to be more suitable for xylose dehydration [201,247]. The maximum yield of furfural (82%) was reported from the reaction with propyl- SO_3H functionalized SBA-15 in toluene- H_2O (1:1) at 170 °C for 20 h [247]. The high catalytic performance can be ascribed to the fast formation of furfural catalyzed by SO_3H sites and the fast diffusion of furfural in the highly ordered mesostructure to avoid secondary reactions [247]. The catalyst after usage lost 40% of SO_3H sites and needed H_2O_2 to remove humins on the catalyst surface [247]. It was found later that by increasing the hydrothermal aging temperature during the co-condensation synthesis, the hydrothermal stability of SO_3H was much improved [244]. The dehydration of xylose in alcoholic medium is different from the consecutive reactions occurred with fructose. It mainly consists of two competitive reactions, xylose etherification to xyloside ethers and xylose dehydration to furfural [245]. The alkyl xyloside acts as a reaction intermediate to form furfural as well in the presence of a Brønsted acid [245].

The obtained furfural can be oxidized to furoic acid or reduced to furfuryl alcohol. Furfuryl alcohol is also an important precursor for many fine and commodity chemicals and fuels (additives), such as 2-methylfuran (MF, sylvan), tetrahydrofurfuryl alcohol and 2-methyltetrahydrofuran [243]. As discussed in the previous synthetic part of this review, furfuryl alcohol is also a widely-applied carbon precursor. In the presence of an acid catalyst in an aqueous solution, furfuryl alcohol will be easily protonated to undergo polymerization through the formation of conjugated diene structures [248]. However, in alcohols, furfuryl alcohol can be atom economically converted to alkyl levulinate [40,45,193,249–252]. The ethanolysis of furfuryl alcohol proceeds through the formation of two intermediates, 2-ethoxy-methylfuran and 4,5,5-triethoxypentan-2-one [252]. Upon optimization of the reaction conditions, a high EL yield up to 95.5% can be obtained with graphene oxide from Hummers method at 120 °C for 6 h [252]. The SO_3H groups are supposed to work synergistically with the co-existing COOH groups, which facilitate the adsorption of furfuryl alcohol [252]. Sulfonated silica-carbon nanocomposites from the pyrolysis of $TsOH-H_2SO_4$ with the template mesoporous silica or fumed silica also showed 79–86% of EL yield in ethanolysis of furfuryl alcohol at 110 °C [40,45]. It is suggested that a combination of high surface area, high amount of acid sites and strong acid strength favour the formation of EL from furfuryl alcohol [40,45]. Guo and co-workers obtained *ca.* 80% of EL at 120 °C with soft-templated $ArSO_3H$ or $PrSO_3H$ modified hollow silica nanospheres, and they emphasized a facilitated mass transfer [250,251]. The catalysts gradually deactivated due to the adsorption of carbonaceous by-products, and those with more

hydrophobic moiety in the structure can reduce the adsorption of polar by-products, thus improving the catalytic stability [250,251]. They also tested sulfonated mesoporous carbon nanospheres and obtained 81% of EL yield at 120 °C after 2 h [193]. The excellent catalytic activity was explained from the strong Brønsted acidity and the hollow nanospherical morphology with thin mesoporous shell [193].

4.2.4. Esterification of levulinic acid to levulinate esters

Levulinate esters formation from the esterification of levulinic acid are also studied, as the products are suitable for fuel additives and have applications in food and perfumes industries [253]. SO_3H functionalized carbon or silica-carbon nanocomposites have been applied for this esterification reaction under mild conditions, showing quite high yields of alkyl levulinate [193,249,250,254–256]. However, some catalysts, such as sulfonated pyrolyzed lignin residues from 5-chloromethylfurfural production (S-LCMF) [254], and sulfonated hydrothermally carbonized rye straw [256], can have a rather low EL selectivity for LA esterification with ethanol. The main side product is attributed to 4-ethoxy- γ -valerolactone [254]. Sulfonated hydrothermally carbonized glucose can have 94% of EL yield at 60 °C for 3 h [256]. The sulfonated pyrolyzed glucose and cellulose, $ArSO_3H$ functionalized ordered mesoporous carbon and $ArSO_3H$ functionalized hollow mesoporous carbon nanospheres were compared in terms of TOF (per acid site) for the esterification of LA to EL [193]. The carbon spheres showed the highest frequency of catalytic turnover, which was ascribed to the strong acidity and the shortest diffusion distance for the reactants and products [193]. The SO_3H -functionalized mesoporous organosilica hybrids also exhibited high levulinate ester yield (> 95%) and they can be recycled more than twice [249,250,255]. The high surface area and pore volume of these mesoporous organosilicas facilitate mass transfer of the reaction [249,250,255]. Besides, the local hydrophobic environment near SO_3H site which reduces the adsorption of the reaction generated H_2O , is thought to promote the esterification of LA [250,255]. Different alcohols were evaluated as well. It was found that the bulkier alcohols such as 2-propanol and 2-butanol decrease the reaction rates due to the steric hindrance effect [255].

4.2.5. Cross-condensation of furan derivatives

Catalytic condensation (with C–C coupling) is also an important class of reactions for biomass valorization, as it eliminates energy-neutral C–O and O–H bonds and creates new C–C bonds of higher energy efficiency [206,257]. Base-catalyzed aldol condensation has been studied a lot, such as HMF or furfural with acetone to form a C_{15} or C_{13} aldol-adduct for the next-step hydrodeoxygenation (HDO) into liquid alkanes [208,257,258]. A similar aldol-type strategy can be performed with 2-methylfuran (MF, sylvan) with carbonyl compounds in the presence of a Brønsted acid, *i.e.*, hydroalkylation and alkylation of sylvan with aldehyde/ketone into bisfurylalkanes [200,217,259–263]. The bisfurylalkanes are intermediates for macromolecular chemistry [200] and precursors for liquid alkane fuels by HDO processing [261,262]. MF can be condensed with a variety of aldehydes or ketones [208,243], such as acetone [200,259,260,262], butanal [262] and furfural [217,261,263]. The steric and electrophilic effects of the substrate carbonyl compounds determine the reactivity with MF for the corresponding bisfurylalkane [262]. The minor product can be formed from MF, hydroalkylated with the *in situ* formed aldehyde (4-oxopentanal from hydrolysis of MF *via* ring opening and keto-enol tautomerism), which is also a C_{15} diesel precursor [261,262]. A few SO_3H functionalized carbon or silica-carbon nanocomposites have been applied to the hydroalkylation/alkylation of MF with different carbonyl compounds, as listed in Table 5. The strong acid site, *viz.* SO_3H , is found to be highly active and selective for the sylvan condensation reaction [262]. Meanwhile, the high surface area [259] or increased hydrophobicity [260] favours the adsorption of non-polar MF and facilitates its conversion. The ordered mesoporous structure allows fast transportation of the substrates and the formed bisfurylalkane,

Table 5
The catalytic reaction results for the hydroxyalkylation/alkylation of MF with different carbonyl compounds.

Catalyst	Preparation procedure	S_{HET} (m^2/g)	^a (mmol/g)	Substrates ^b	T (°C)	t (h)	Cat. ^c (wt %)	Yield (%)	Selectivity (%)	Stability	Ref.
MCM-50	MCM-41 grafted with MPMS and oxidized by H_2O_2	399	Not reported	MF/acetone (1:2.5)	50	24	5.6	82	96	Not reported	[200]
MS-SO ₃ H/390nm	Co-condensation of TMOS ^d and MPMS in the presence of CTAC ^e , removal of surfactant and oxidized by H_2O_2	1000	0.61	MF/acetone (1:2.6)	50	4	5.5	97	99	Not reported	[259]
MS-SO ₃ H/Pr	Co-condensation of TMOS ^f in sequence with MPMS and PrTMS ^f in the presence of CTAC ^e , removal of surfactant and oxidized by H_2O_2	1170	0.63	MF/acetone (1:2.6)	50	2	5.5	72	Not reported	Not reported	[260]
CMK-3-SO ₃ H-250	Hard template synthesis with SBA-15 and sucrose, pyrolyzed at 900 °C, removal of SiO ₂ , and sulfonated in concentrated H ₂ SO ₄	412	0.63	MF/butanal (2:1)	50	2	10.4	66	76	Not reported	[161,262]
MC-SO ₃ H-250	Soft template synthesis of resorcinol/Fl27, pyrolyzed at 800 °C, and sulfonated in concentrated H ₂ SO ₄	834	0.28	MF/butanal (2:1)	50	2	10.4	54	78	Not reported	[161,262]
LF	Sodium ligosulfonate exchanged with 2 M H ₂ SO ₄ solution	2	1.02	MF/furfural (2:1)	50	2	7.8	65	93	Stable	[261]
CMH-200-1273-SO ₃ H	Resorcinol-formaldehyde resin aerogel pyrolyzed at 1000 °C, and sulfonated in concentrated H ₂ SO ₄	570	0.62	MF/furfural (2:2.1)	45	9	16.8	64	90	Stable	[217]
7c	Silica gel grafted with 3-(3-trimethoxysilylpropyl)thiopropane-1-sulfonic acid, and oxidized by H_2O_2	267	0.61	MF/furfural (2:2.1)	65	2	85.2	89	89	Stable	[263]

^a Represents the SO₃H group density in the catalyst.

^b The ratio in the brackets is the molar ratio of MF and the carbonyl compound.

^c Cat. indicates the catalyst loading relative to the carbonyl compound.

^d TMOS is tetramethoxysilane.

^e CTAC is cetyltrimethylammonium chloride.

^f PrTMS is propyltrimethoxysilane.

leading to a high TOF [217,262]. The spent SO₃H functionalized carbon or silica-carbon materials did not show severe deactivation in successive runs.

5. Conclusions and future outlook

Sulfonated ordered mesoporous carbon or silica-carbon nanocomposites have attracted great research interest in the past decades due to their excellent physicochemical properties. For synthesis of the mesoporous structure, hard-template (nanocasting from the pre-formed hard templates) and soft-template (direct formation of mesostructure induced by assembly of co-polymer surfactants) strategies are available. Soft templating method owns the merits of avoiding a multiple-step process (and a sacrifice of template) and of time-saving. Among direct soft-template syntheses, 6 routes including EISA, EIAA, macrophase separation, hydrothermal processing, dilute solution and solution-phase synthesis for the composite are summarized. Each methodology has specific merits as well as weakness. Generally, EISA is an ingenious method to fabricate ordered mesoporous carbon or silica-carbon nanocomposites material upon fast evaporation of the solvent and concentration of the surfactant. The precursors can be rapidly “locked” in the vicinity of the micelles; for example, partly hydrolyzed TEOS oligomers and phenol-formaldehyde oligomers aggregates in the PEO domain of F127 micelles with the drive force of H-bonding. Therefore, this method is especially suitable for silica-carbon nanocomposite synthesis due to a uniform distribution of carbon and silica phases. However, to realize fast evaporation of the solvent with the traditional EISA method through thin-film is laborious and hard to scale-up. This problem can be addressed by using an alternative rapid rotary-evaporation induced self-assembly (ROT-EISA) method [264]. The solution-phase synthetic methods are also interesting, but they usually create more defects in the structure and may require high energy consumption as in the case of hydrothermal processing.

Concerning the carbon precursor in the soft-template synthesis, phenolic derivatives have been utilized a lot but they are not as cheap and green as biomass-derived carbohydrates like sucrose [68,265]. As a potential substitute, sucrose similarly possesses abundant hydroxyl groups for H-bonding with micelles and siliceous species. Furthermore, during the pyrolysis or hydrothermal carbonization, sucrose can produce a number of furan derivatives, which finally turn into thermally or hydrothermally stable carbon phase in the structure.

Built-in and post-synthetic ways of introducing SO₃H groups to carbonaceous surface are reviewed. To ensure the ordered mesoporous structure of the material, post-synthetic functionalization is more commonly adopted. Concentrated or fuming H₂SO₄, ClSO₃H, 4-benzene-diazoniumsulfonate and S-containing organosilanes have been used as sulfonation agents. Concentrated H₂SO₄ is the most economically favourable. However, for a high loading of SO₃H sites, it requires an elevated treatment temperature. Thus, the structure needs to be robust enough to avoid deterioration. In this context, mesoporous silica-carbon nanocomposites are preferred over pure mesoporous carbon framework to be subjected to sulfonation in concentrated H₂SO₄.

The SO₃H-functionalized mesostructured carbon or silica-carbon nanocomposites have demonstrated promising behaviours in catalytic transformation of biomass-derived compounds into value-added products. They are typical strong Brønsted solid acids, which can be applied to esterification of fatty acids, transesterification of triglycerides, hydrolysis of cellulose, dehydration of monosaccharides, condensation of MF and so on. Their well-ordered mesoporous structure provides a large surface area for the interaction with reactants and uniform mesopores for facile diffusion of reactants and products. Meanwhile the surface is amphiphilic with tuneable hydrophilicity (C—S O₃H, C—OH, C—COOH and Si—OH in a silica-carbon nanocomposite) and hydrophobicity (polyaromatic hydrocarbon). By the unlimited accessibility to SO₃H acid sites and well-controlled surface polarity balance, a high catalytic performance can be expected for this sort of acid-catalyzed

biomass transformation reactions.

Our group has studied the synthesis of mesoporous silica-carbon nanocomposites with the approach of EISA of tri-constituents (sucrose as carbon precursor, TEOS as silica precursor and F127 as the structure-directing soft template) [68,265]. Applying the SiO₂ component in the synthesis not only facilitates the co-assembly upon evaporation of solvent, but also declines the framework shrinkage during the carbonization step. The insights into the entangled nanosized silica or carbon phases in the composite were provided by analyzing the derived pure carbon or pure silica structure [265]. The sulfonation of the mesoporous silica-carbon material was carried out directly in concentrated H₂SO₄, owing to the improved stability by SiO₂. Different silica/sucrose weight ratios (Si₃₃C₆₆, Si₅₀C₅₀ and Si₆₆C₃₃), and different pyrolysis temperatures (400 and 550 °C) were employed, offering different SO₃H amounts and strengths and different textural and surface properties. This series of sulfonated mesoporous silica-carbon nanocomposites allow a systematic study for the influencing factors in styrene and α -methylstyrene dimerization reaction [265], cellulose hydrolysis [68], and fructose ethanolysis [266].

From the viewpoint of both fundamental research and practical applications, much effort is still required for the improvement of the synthesis and functionalization of mesoporous silica-carbon nanocomposites. Many biomass-related reactions, such as those in Fig. 12 not affected by the Brønsted acid catalysis, require other type of catalytically active functionalities or multi-functionalities to realize one-pot cascade conversions. Based on the TEOS-sucrose-F127 synthesis system, the following perspectives can therefore be considered:

- I Other carbon precursors, activating agents or mixtures of carbon precursors with different functionalities may be applied for the synthesis. For example, using hexamine can increase the cross-linking degree of carbon phase and introduce N sites, with basic (or generally more electron-donating) properties, to the material.
- II Other inorganic precursors for Al, Zr, Ti, Sn and so on, may be used partly or completely replace TEOS. For instance, aluminum 2-propoxide is quite similar to TEOS, and Al creates Lewis acid sites in the material, being able for instance to catalyze the carbonization process, or useful for catalytic applications.
- III Other metallic nanoparticles or their precursor salts can be involved in the synthesis to be incorporated in the mesostructure. For example, PdCl₂ and NiCl₂ may be hydrolyzed together with silicates and reduced during the synthesis to realize a high dispersion of metal nanoparticles for catalysis, e.g., hydrogenation or oxidation reactions.
- IV The dry pyrolysis can be changed into a hydrothermal carbonization. The hydrothermal carbonization may result in a better preserved mesostructure, a strengthened interaction between silica and carbon phases, and a higher content of oxygenated groups on the carbon surface.
- V The post-synthetic modification of surface and structure is also possible, such as grafting of Lewis acid Sn sites.

The versatility of fabricating functionalized mesoporous carbonaceous materials has a high potential in several applications like the valorization of biomass. These materials aim at providing abundant accessible (multi-)active sites for the transformation, the well-ordered mesochannels for fast mass transfer of sterically demanding molecules, and high hydrothermal stability arising from the carbon phase in the framework. All these aspects will help to solve the current bottle-neck problems in biomass valorization and promote the sustainable development of the society. Especial attention should go to stability of the catalysts and to discover easy ways to either avoid fouling of the active sites or to regenerate such spent carbon catalysts.

Acknowledgments

R.Z. acknowledges the Chinese Scholarship Council (No. 201206210307) for financial support.

References

- [1] M.E. Davis, *Nature* 417 (2002) 813–821.
- [2] A. Corma, *Chem. Rev.* 97 (1997) 2373–2419.
- [3] D. Zhao, J. Feng, Q. Huo, N. Melosh, G.H. Fredrickson, B.F. Chmelka, G.D. Stucky, *Science* 279 (1998) 548–552.
- [4] A. Dewaele, F. Verpoort, B. Sels, *ChemCatChem* 8 (2016) 3010–3030.
- [5] Q. Yang, J. Liu, L. Zhang, C. Li, *J. Mater. Chem.* 19 (2009) 1945–1955.
- [6] N. Pal, A. Bhaumik, *RSC Adv.* 5 (2015) 24363–24391.
- [7] P. Bhanja, A. Bhaumik, *Fuel* 185 (2016) 432–441.
- [8] U. Diaz, D. Brunel, A. Corma, *Chem. Soc. Rev.* 42 (2013) 4083–4097.
- [9] A. Taguchi, F. Schuth, *Microporous Mesoporous Mater.* 77 (2005) 1–45.
- [10] F. Chen, X. Meng, F. Xiao, *Catal. Surv. Asia* 15 (2011) 37–48.
- [11] Z. Tai, A.F. Lee, K. Wilson, *Reaction Pathways and Mechanisms in Thermocatalytic Biomass Conversion I: Cellulose Structure, Depolymerization and Conversion by Heterogeneous Catalysts*, Springer, Singapore, 2016, pp. 123–169.
- [12] Z. Wu, D. Zhao, *Chem. Commun.* 47 (2011) 3332–3338.
- [13] M. Hartmann, *Chem. Mater.* 17 (2005) 4577–4593.
- [14] Y. Zhai, Y. Dou, D. Zhao, P.F. Fulvio, R.T. Mayes, S. Dai, *Adv. Mater.* 23 (2011) 4828–4850.
- [15] M.C. Oriall, U. Wiesner, *Chem. Soc. Rev.* 40 (2011) 520–535.
- [16] L. Nicole, C. Laberty-Robert, L. Rozes, C. Sanchez, *Nanoscale* 6 (2014) 6267–6292.
- [17] M. Manzano, M. Vallet-Regi, *J. Mater. Chem.* 20 (2010) 5593–5604.
- [18] B.J. Scott, G. Wirsberger, G.D. Stucky, *Chem. Mater.* 13 (2001) 3140–3150.
- [19] T. Tran-Thi, R. Dagnelie, S. Crunaire, L. Nicole, *Chem. Soc. Rev.* 40 (2011) 621–639.
- [20] F. de Clippel, M. Dusselier, S. Van de Vyver, L. Peng, P.A. Jacobs, B.F. Sels, *Green Chem.* 15 (2013) 1398–1430.
- [21] J. Matthiesen, T. Hoff, C. Liu, C. Pueschel, R. Rao, J. Tessonner, *Chin. J. Catal.* 35 (2014) 842–855.
- [22] J.A. Melero, R. van Grieken, G. Morales, *Chem. Rev.* 106 (2006) 3790–3812.
- [23] F. Hoffmann, M. Froba, *Chem. Soc. Rev.* 40 (2011) 608–620.
- [24] F. Hoffmann, M. Cornelius, J. Morell, M. Froba, *Angew. Chem. Int. Ed.* 45 (2006) 3216–3251.
- [25] P. Van Der Voort, D. Esquivel, E. De Canck, F. Goethals, I. Van Driessche, F.J. Romero-Salguero, *Chem. Soc. Rev.* 42 (2013) 3913–3955.
- [26] Y. Wan, Y.F. Shi, D. Zhao, *Chem. Mater.* 20 (2008) 932–945.
- [27] T. Ma, L. Liu, Z. Yuan, *Chem. Soc. Rev.* 42 (2013) 3977–4003.
- [28] M. Enterria, J.L. Figueiredo, *Carbon* 108 (2016) 79–102.
- [29] X. Sun, R. Wang, D. Su, *Chin. J. Catal.* 34 (2013) 508–523.
- [30] C. Liang, Z. Li, S. Dai, *Angew. Chem. Int. Ed.* 47 (2008) 3696–3717.
- [31] W. Xin, Y. Song, *RSC Adv.* 5 (2015) 83239–83285.
- [32] A. Stein, Z. Wang, M.A. Fierke, *Adv. Mater.* 21 (2009) 265–293.
- [33] R. Ryoo, S.H. Joo, S. Jun, *J. Phys. Chem. B* 103 (1999) 7743–7746.
- [34] M. Inagaki, M. Toyoda, Y. Soneda, S. Tsujimura, T. Morishita, *Carbon* 107 (2016) 448–473.
- [35] J. Lee, S. Yoon, S.M. Oh, C. Shin, T. Hyeon, *Adv. Mater.* 12 (2000) 359–362.
- [36] J. Lee, S. Yoon, T. Hyeon, S.M. Oh, K. Bum Kim, *Chem. Commun.* 35 (1999) 2177–2178.
- [37] J. Janaun, N. Ellis, *Appl. Catal. A* 394 (2011) 25–31.
- [38] P. Valle-Vigon, M. Sevilla, A.B. Fuertes, *Appl. Surf. Sci.* 261 (2012) 574–583.
- [39] L. Fang, K. Zhang, X.H. Li, H.H. Wu, P. Wu, *Chin. J. Catal.* 33 (2012) 114–122.
- [40] P.A. Russo, M.M. Antunes, P. Neves, P.V. Wiper, E. Fazio, F. Neri, F. Barreca, L. Mafra, M. Pillinger, N. Pinna, A.A. Valente, *Green Chem.* 16 (2014) 4292–4305.
- [41] K. Nakajima, M. Okamura, J.N. Kondo, K. Domon, T. Tatsumi, S. Hayashi, M. Hara, *Chem. Mater.* 21 (2009) 186–193.
- [42] F. de Clippel, A. Harkiolakis, X. Ke, T. Bosch, G. Van Tendeloo, G.V. Baron, P.A. Jacobs, J.F.M. Denayer, B.F. Sels, *Chem. Commun.* 46 (2010) 928–930.
- [43] R. Liu, Y. Shi, Y. Wan, Y. Meng, F. Zhang, D. Gu, Z. Chen, B. Tu, D. Zhao, *J. Am. Chem. Soc.* 128 (2006) 11652–11662.
- [44] Y. Zhai, B. Tu, D. Zhao, *J. Mater. Chem.* 19 (2009) 131–140.
- [45] P.A. Russo, M.M. Antunes, P. Neves, P.V. Wiper, E. Fazio, F. Neri, F. Barreca, L. Mafra, M. Pillinger, N. Pinna, A.A. Valente, *J. Mater. Chem. A* 2 (2014) 11813–11824.
- [46] B. Du, X. Zhang, L. Lou, Y. Dong, G. Liu, S. Liu, *Appl. Surf. Sci.* 258 (2012) 7166–7173.
- [47] I. Maria, M. Vera, P. Cool, H. Valeria, *Rev. Roum. Chim.* 59 (2014) 593–597.
- [48] F. de Clippel, M. Dusselier, R. Van Rompaey, P. Vanelderen, J. Dijkmans, E. Makshina, L. Giebel, S. Oswald, G.V. Baron, J.F.M. Denayer, P.P. Pescarmona, P.A. Jacobs, B.F. Sels, *J. Am. Chem. Soc.* 134 (2012) 10089–10101.
- [49] B. Chang, J. Fu, Y. Tian, X. Dong, *J. Phys. Chem. C* 117 (2013) 6252–6258.
- [50] H. Nishihara, Y. Fukura, K. Inde, K. Tsuji, M. Takeuchi, T. Kyotani, *Carbon* 46 (2008) 48–53.
- [51] P. Valle-Vigon, M. Sevilla, A.B. Fuertes, *Mater. Chem. Phys.* 139 (2013) 281–289.
- [52] X. Yan, B. Xu, *J. Mater. Chem. A* 2 (2014) 8617–8622.
- [53] B. Karimi, H.M. Mirzaei, H. Behzadnia, H. Vali, A.C.S. Appl. Mater. Inter. 7 (2015) 19050–19059.
- [54] M. Choi, F. Kleitz, D. Liu, H.Y. Lee, W. Ahn, R. Ryoo, *J. Am. Chem. Soc.* 127 (2005) 1924–1932.
- [55] B. Karimi, M.R. Marefat, M. Hasannia, P.F. Akhavan, F. Mansouri, Z. Artelli, F. Mohammadi, H. Vali, *ChemCatChem* 8 (2016) 2508–2515.
- [56] J. Li, Y. Liang, B. Dou, C. Ma, R. Lu, Z. Hao, Q. Xie, Z. Luan, K. Li, *Mater. Chem. Phys.* 138 (2013) 484–489.
- [57] S. Banerjee, T.K. Paira, A. Kotal, T.K. Mandal, *Adv. Funct. Mater.* 22 (2012) 4751–4762.
- [58] M.H. Lim, A. Stein, *Chem. Mater.* 11 (1999) 3285–3295.
- [59] P. Gupta, S. Paul, *Green Chem.* 13 (2011) 2365–2372.
- [60] S. Kubo, R. Demir-Cakan, L. Zhao, R.J. White, M. Titirici, *ChemSusChem* 3 (2010) 188–194.
- [61] Y. Meng, D. Gu, F. Zhang, Y. Shi, H. Yang, Z. Li, C. Yu, B. Tu, D. Zhao, *Angew. Chem. Int. Ed.* 44 (2005) 7053–7059.
- [62] C. Liang, S. Dai, *J. Am. Chem. Soc.* 128 (2006) 5316–5317.
- [63] C. Liang, K. Hong, G.A. Guiochon, J.W. Mays, S. Dai, *Angew. Chem. Int. Ed.* 43 (2004) 5785–5789.
- [64] P. Valle-Vigon, M. Sevilla, A.B. Fuertes, *Micropor. Mesoporous Mater.* 134 (2010) 165–174.
- [65] J. Kim, J. Lee, T. Hyeon, *Carbon* 42 (2004) 2711–2719.
- [66] Q. Yue, M. Wang, J. Wei, Y. Deng, T. Liu, R. Che, B. Tu, D. Zhao, *Angew. Chem. Int. Ed.* 51 (2012) 10368–10372.
- [67] L. Chuenchom, R. Krahnert, B.M. Smarsly, *Soft Matter* 8 (2012) 10801–10812.
- [68] S. Van de Vyver, L. Peng, J. Geboers, H. Schepers, F. de Clippel, C.J. Gommes, B. Goderis, P.A. Jacobs, B.F. Sels, *Green Chem.* 12 (2010) 1560–1563.
- [69] Y. Wan, D. Zhao, *Chem. Rev.* 107 (2007) 2821–2860.
- [70] J.L. Blin, M. Imperor-Clerc, *Chem. Soc. Rev.* 42 (2013) 4071–4082.
- [71] C.J. Brinker, Y.F. Lu, A. Sellinger, H.Y. Fan, *Adv. Mater.* 11 (1999) 579–585.
- [72] W. Li, D. Zhao, *Chem. Commun.* (2013) 943–946.
- [73] X. Wang, C. Liang, S. Dai, *Langmuir* 24 (2008) 7500–7505.
- [74] S. Schlienger, A. Graff, A. Celzard, J. Parmentier, *Green Chem.* 14 (2012) 313–316.
- [75] N. Pal, A. Bhaumik, *Adv. Colloid Interface Sci.* 189–190 (2013) 21–41.
- [76] S. Tanaka, N. Nishiyama, Y. Egashira, K. Ueyama, *Chem. Commun.* (2005) 2125–2127.
- [77] A.T. Rodriguez, X. Li, J. Wang, W.A. Steen, H. Fan, *Adv. Funct. Mater.* 17 (2007) 2710–2716.
- [78] Y.F. Lu, R. Ganguli, C.A. Drewien, M.T. Anderson, C.J. Brinker, W.L. Gong, Y.X. Guo, H. Soyez, B. Dunn, M.H. Huang, J.I. Zink, *Nature* 389 (1997) 364–368.
- [79] D. Zhao, P. Yang, N. Melosh, J. Feng, B.F. Chmelka, G.D. Stucky, *Adv. Mater.* 10 (1998) 1380–1385.
- [80] S. Kataoka, T. Yamamoto, A. Endo, M. Nakaiwa, T. Ohmori, *Colloids Surf. A* 347 (2009) 142–145.
- [81] Y. Meng, D. Gu, F. Zhang, Y. Shi, L. Cheng, D. Feng, Z. Wu, Z. Chen, Y. Wan, A. Stein, D. Zhao, *Chem. Mater.* 18 (2006) 4447–4464.
- [82] W. Li, Q. Yue, Y. Deng, D. Zhao, *Adv. Mater.* 25 (2013) 5129–5152.
- [83] D. Gross, F. Cagnol, G.J.D.A. Soler-Illia, E.L. Crepaldi, H. Amenitsch, A. Brunet-Brunneau, A. Bourgeois, C. Sanchez, *Adv. Funct. Mater.* 14 (2004) 309–322.
- [84] A. Gibaud, D. Gross, B. Smarsly, A. Baptiste, J.F. Bardeau, F. Babonneau, D.A. Doshi, Z. Chen, C.J. Brinker, C. Sanchez, *J. Phys. Chem. B* 107 (2003) 6114–6118.
- [85] I. Muylaert, A. Verberckmoes, J. De Decker, P. Van Der Voort, *Adv. Colloid Interface Sci.* 175 (2012) 39–51.
- [86] C. Matei Ghimbeu, L. Vidal, L. Delmotte, J. Le Meins, C. Vix-Guterl, *Green Chem.* 16 (2014) 3079–3088.
- [87] C. Xue, B. Tu, D. Zhao, *Adv. Funct. Mater.* 18 (2008) 3914–3921.
- [88] M. Florent, C. Xue, D. Zhao, D. Goldfarb, *Chem. Mater.* 24 (2012) 383–392.
- [89] H. Wei, Y. Lv, L. Han, B. Tu, D. Zhao, *Chem. Mater.* 23 (2011) 2353–2360.
- [90] Z. Qiang, Y. Guo, H. Liu, S.Z.D. Cheng, M. Cakmak, K.A. Cavicchi, B.D. Vogt, *ACS Appl. Mater. Interfaces* 7 (2015) 4306–4310.
- [91] Q. Hu, R. Kou, J. Pang, T.L. Ward, M. Cai, Z. Yang, Y. Lu, J. Tang, *Chem. Commun.* 43 (2007) 601–603.
- [92] Y. Li, J. Wei, W. Luo, C. Wang, W. Li, S. Feng, Q. Yue, M. Wang, A.A. Elzatahry, Y. Deng, D. Zhao, *Chem. Mater.* 26 (2014) 2438–2444.
- [93] J. Xu, A. Wang, T. Zhang, *Carbon* 50 (2012) 1807–1816.
- [94] B. Chang, J. Fu, Y. Tian, X. Dong, *RSC Adv.* 3 (2013) 1987–1994.
- [95] J. Gorka, M. Jaroniec, *J. Phys. Chem. C* 114 (2010) 6298–6303.
- [96] Y. Fang, D. Gu, Y. Zou, Z. Wu, F. Li, R. Che, Y. Deng, B. Tu, D. Zhao, *Angew. Chem. Int. Ed.* 49 (2010) 7987–7991.
- [97] J. Wei, Y. Liang, X. Zhang, G.P. Simon, D. Zhao, J. Zhang, S. Jiang, H. Wang, *Nanoscale* 7 (2015) 6247–6254.
- [98] S. Feng, W. Li, J. Wang, Y. Song, A.A. Elzatahry, Y. Xia, D. Zhao, *Nanoscale* 6 (2014) 14657–14661.
- [99] L. Liu, F. Wang, G. Shao, Z. Yuan, *Carbon* 48 (2010) 2089–2099.
- [100] S. Kubo, R.J. White, N. Yoshizawa, M. Antonietti, M. Titirici, *Chem. Mater.* 23 (2011) 4882–4885.
- [101] F. Liu, C. Li, L. Ren, X. Meng, H. Zhang, F. Xiao, *J. Mater. Chem.* 19 (2009) 7921–7928.
- [102] F. Liu, S. Zuo, W. Kong, C. Qi, *Green Chem.* 14 (2012) 1342–1349.
- [103] D. Liu, J. Lei, L. Guo, K. Deng, *Carbon* 49 (2011) 2113–2119.
- [104] F. Zhang, Y. Meng, D. Gu, Y. Yan, Z. Chen, B. Tu, D. Zhao, *Chem. Mater.* 18 (2006) 5279–5288.
- [105] F. Zhang, Y. Meng, D. Gu, C. Yan, B. Yu, D. Tu, D. Zhao, *J. Am. Chem. Soc.* 127 (2005) 13508–13509.
- [106] D. Liu, J. Lei, L. Guo, D. Qu, Y. Li, B. Su, *Carbon* 50 (2012) 476–487.
- [107] J. Lee, J. Kim, Y. Lee, S. Yoon, S.M. Oh, T. Hyeon, *Chem. Mater.* 16 (2004) 3323–3330.
- [108] L. Li, H. Song, X. Chen, *Microporous Mesoporous Mater.* 94 (2006) 9–14.

[109] C. Ting, H. Wu, S. Vetrivel, D. Saikia, Y. Pan, G.T.K. Fey, H. Kao, Microporous Mesoporous Mater. 128 (2010) 1–11.

[110] C. Ting, Y. Pan, S. Vetrivel, D. Saikia, H. Kao, RSC Adv. 2 (2012) 2221–2224.

[111] N. Liu, H. Song, X. Chen, J. Mater. Chem. 21 (2011) 5345–5351.

[112] X. Yan, H. Song, X. Chen, J. Mater. Chem. 19 (2009) 4491–4494.

[113] S. Polzari, B. Smarsly, L. Bronstein, M. Antonietti, Angew. Chem. 40 (2001) 4549–4553.

[114] Y. Deng, C. Liu, T. Yu, F. Liu, F. Zhang, Y. Wan, L. Zhang, C. Wang, B. Tu, P.A. Webley, H. Wang, D. Zhao, Chem. Mater. 19 (2007) 3271–3277.

[115] M. Jaroniec, J. Gorka, J. Choma, A. Zawislak, Carbon 47 (2009) 3034–3040.

[116] X. Zhang, L. Zhang, Q. Yang, J. Mater. Chem. A 2 (2014) 7546–7554.

[117] J. Chen, J. Chen, X. Zhang, J. Gao, Q. Yang, Appl. Catal. A 516 (2016) 1–8.

[118] B. Guan, X. Wang, Y. Xiao, Y. Liu, Q. Huo, Nanoscale 5 (2013) 2469–2475.

[119] C. Xue, B. Tu, D. Zhao, Nano Res. 2 (2009) 242–253.

[120] A.T. Rodriguez, M. Chen, Z. Chen, C.J. Brinker, H. Fan, J. Am. Chem. Soc. 128 (2006) 9276–9277.

[121] D. Shao, D. Tang, Y. Mai, L. Zhang, J. Mater. Chem. A 1 (2013) 15068–15075.

[122] K. Nakajima, M. Hara, ACS Catal. 2 (2012) 1296–1304.

[123] M. Okamura, A. Takagaki, M. Toda, J.N. Kondo, K. Domen, T. Tatsumi, M. Hara, S. Hayashi, Chem. Mater. 18 (2006) 3039–3045.

[124] K. Fukuhara, K. Nakajima, M. Kitano, H. Kato, S. Hayashi, M. Hara, ChemSusChem 4 (2011) 778–784.

[125] K. Nakajima, M. Hara, S. Hayashi, J. Am. Ceram. Soc. 90 (2007) 3725–3734.

[126] R.J. White, V. Budarin, R. Luque, J.H. Clark, D.J. Macquarrie, Chem. Soc. Rev. 38 (2009) 3401–3418.

[127] V. Budarin, J.H. Clark, J.J.E. Hardy, R. Luque, K. Milkowski, S.J. Tavener, A.J. Wilson, Angew. Chem. Int. Ed. 45 (2006) 3782–3786.

[128] W. Lou, Q. Guo, W. Chen, M. Zong, H. Wu, T.J. Smith, ChemSusChem 5 (2012) 1533–1541.

[129] S. Satohi, N. Kiyotaka, K. Masaaki, Y. Daizo, K. Hideki, H. Shigenobu, M. Hara, J. Am. Chem. Soc. 130 (2008) 12787–12793.

[130] Y. Zhai, Y. Wan, Y. Cheng, Y. Shi, F. Zhang, B. Tu, D. Zhao, J. Porous Mater. 15 (2008) 601–611.

[131] L. Song, D. Feng, N.J. Fredin, K.G. Yager, R.L. Jones, Q. Wu, D. Zhao, B.D. Vogt, ACS Nano 4 (2010) 189–198.

[132] L. Song, D. Feng, H. Lee, C. Wang, Q. Wu, D. Zhao, B.D. Vogt, J. Phys. Chem. C 114 (2010) 9618–9626.

[133] Z. Yang, Y. Xia, R. Mokaya, J. Mater. Chem. 16 (2006) 3417–3425.

[134] J. Pang, V.T. John, D.A. Loy, Z. Yang, Y. Lu, Adv. Mater. 17 (2005) 704–707.

[135] T. Mochizuki, D. Atong, S. Chen, M. Toba, Y. Yoshimura, Catal. Commun. 36 (2013) 1–4.

[136] M. Titirici, R.J. White, C. Falco, M. Sevilla, Energy Environ. Sci. 5 (2012) 6796–6822.

[137] J.A. Libra, K.S. Ro, C. Kammann, A. Funke, N.D. Berge, Y. Neubauer, M. Titirici, C. Fühner, O. Bens, J. Kern, K. Emmerich, Biofuels 2 (2010) 71–106.

[138] M. Sevilla, A.B. Fuertes, Chem. Eur. J. 15 (2009) 4195–4203.

[139] M. Liu, S. Jia, Y. Gong, C. Song, X. Guo, Ind. Eng. Chem. Res. 52 (2013) 8167–8173.

[140] Y.J. Jiang, X.T. Li, Q.A. Cao, X.D. Mu, J. Nanopart. Res. 13 (2011) 463–469.

[141] J.M. Fraile, E. Garcia-Bordeje, L. Roldan, J. Catal. 289 (2012) 73–79.

[142] M. Titirici, M. Antonietti, N. Baccile, Green Chem. 10 (2008) 1204.

[143] M. Zhang, H. Yang, Y. Liu, X. Sun, D. Zhang, D. Xue, Carbon 50 (2012) 2155–2161.

[144] S. Kang, J. Ye, Y. Zhang, J. Chang, RSC Adv. 3 (2013) 7360–7366.

[145] M. Titirici, A. Thomas, M. Antonietti, J. Mater. Chem. 17 (2007) 3412–3418.

[146] L. Yu, N. Brun, K. Sakaushi, J. Eckert, M.M. Titirici, Carbon 61 (2013) 245–253.

[147] P. Gupta, S. Paul, Catal. Today 236 (2014) 153–170.

[148] J.A. Melero, J. Iglesias, G. Morales, Green Chem. 11 (2009) 1285–1308.

[149] R. Fernandez-Prini, P. Schulman, J. Appl. Polym. Sci. 29 (1984) 341–352.

[150] W. Zhang, H. Tao, B. Zhang, J. Ren, G. Lu, Y. Wang, Carbon 49 (2011) 1811–1820.

[151] B. Zhang, J. Ren, X. Liu, Y. Guo, Y. Guo, G. Lu, Y. Wang, Catal. Commun. 11 (2010) 629–632.

[152] J. Wang, W. Xu, J. Ren, X. Liu, G. Lu, Y. Wang, Green Chem. 13 (2011) 2678–2681.

[153] R. Jia, J. Ren, X. Liu, G. Lu, Y. Wang, J. Mater. Chem. A 2 (2014) 11195–11201.

[154] X. Liang, M. Zeng, C. Qi, Carbon 48 (2010) 1844–1848.

[155] M. Hara, T. Yoshida, A. Takagaki, T. Takata, J.N. Kondo, S. Hayashi, K. Domen, Angew. Chem. Int. Ed. 43 (2004) 2955–2958.

[156] A. Takagaki, M. Toda, M. Okamura, J.N. Kondo, S. Hayashi, K. Domen, M. Hara, Catal. Today 116 (2006) 157–161.

[157] Z. Hasan, J. Hwang, S.H. Jhung, Catal. Commun. 26 (2012) 30–33.

[158] X.L. Song, X.B. Fu, C.W. Zhang, W.Y. Huang, Y. Zhu, J. Yang, Y.M. Zhang, Catal. Lett. 142 (2012) 869–874.

[159] D. Nandan, P. Sreenivasulu, S.K. Saxena, N. Viswanadham, Chem. Commun. 47 (2011) 11537–11539.

[160] D. Nandan, P. Sreenivasulu, L.N. Sivakumar Konathala, M. Kumar, N. Viswanadham, Microporous Mesoporous Mater. 179 (2013) 182–190.

[161] J. Pang, A. Wang, M. Zheng, T. Zhang, Chem. Commun. 46 (2010) 6935–6937.

[162] S. Saravanamurugan, A. Riisager, Catal. Commun. 17 (2012) 71–75.

[163] M.H. Tucker, A.J. Crisci, B.N. Wigington, N. Phadke, R. Alamillo, J. Zhang, S.L. Scott, J.A. Dumesic, ACS Catal. 2 (2012) 1865–1876.

[164] G. Morales, G. Athens, B.F. Chmelka, R.V. Grieken, J.A. Melero, J. Catal. 254 (2008) 205–217.

[165] G. Morales, M. Paniagua, J.A. Melero, J. Iglesias, Catal. Today 279 (2017) 305–316.

[166] X. Zhuang, Q. Zhao, Y. Wan, J. Mater. Chem. 20 (2010) 4715–4724.

[167] W. Wang, X. Zhuang, Q.F. Zhao, Y. Wan, J. Mater. Chem. A 22 (2012) 15874–15886.

[168] J.V. de Assis, P.A.S. Abranches, I.B. Braga, O.M.P. Zuniga, A.G. Sathicq, G.P. Romanelli, A.G. Sato, S.A. Fernandes, RSC Adv. 6 (2016) 24285–24289.

[169] I. Sadaba, M. Ojeda, R. Mariscal, M.L. Granados, Appl. Catal. B 150–151 (2014) 421–431.

[170] M. Toda, A. Takagaki, M. Okamura, J.N. Kondo, S. Hayashi, K. Domen, M. Hara, Nature 438 (2005) 178.

[171] X. Mo, D.E. Lopez, K. Suwannakarn, Y. Liu, E. Lotero, J.G. Goodwin Jr, C. Lu, J. Catal. 254 (2008) 332–338.

[172] J.R. Kastner, J. Miller, D.P. Geller, J. Locklin, L.H. Keith, T. Johnson, Catal. Today 190 (2012) 122–132.

[173] X. Dong, Y. Jiang, W. Shan, M. Zhang, RSC Adv. 6 (2016) 17118–17124.

[174] I.M. Lokman, U. Rashid, Y.H. Taufiq-Yap, R. Yunus, Renew. Energy 81 (2015) 347–354.

[175] K. Hou, A. Zhang, L. Gu, M. Liu, X. Guo, J. Colloid Interface Sci. 377 (2012) 18–26.

[176] L. Peng, A. Philippaerts, X. Ke, J. Van Noyen, F. De Clippe, G. Van Tendeloo, P.A. Jacobs, B.F. Sels, Catal. Today 150 (2010) 140–146.

[177] C. Poonjarernsilp, N. Sano, H. Tamon, Appl. Catal. B 147 (2014) 726–732.

[178] R. Xing, N. Liu, Y. Liu, H. Wu, Y. Jiang, L. Chen, M. He, P. Wu, Adv. Funct. Mater. 17 (2007) 2455–2461.

[179] R. Xing, Y. Liu, Y. Wang, L. Chen, H. Wu, Y. Jiang, M. He, P. Wu, Microporous Mesoporous Mater. 105 (2007) 41–48.

[180] K. Nakajima, I. Tomita, M. Hara, S. Hayashi, K. Domen, Adv. Mater. 17 (2005) 1839–1842.

[181] S. Chu, G. Cai, Z. Tan, D. Xiang, C. Xiong, New J. Chem. 40 (2016) 1957–1961.

[182] C. Bispo, K. De Oliveira Vigier, M. Sardo, N. Bion, L. Mafra, P. Ferreira, F. Jerome, Catal. Sci. Technol. 4 (2014) 2235–2240.

[183] Y. Liu, J. Chen, J. Yao, Y. Lu, L. Zhang, X. Liu, Chem. Eng. J. 148 (2009) 201–206.

[184] Z. Zhang, Y. Wang, Z. Fang, B. Liu, ChemPlusChem 79 (2014) 233–240.

[185] Z. Yuan, Z. Zhang, J. Zheng, J. Lin, Fuel 150 (2015) 236–242.

[186] M. Balakrishnan, E.R. Sacia, A.T. Bell, Green Chem. 14 (2012) 1626–1634.

[187] L. Wang, J. Zhang, S. Yang, Q. Sun, L. Zhu, Q. Wu, H. Zhang, X. Meng, F. Xiao, J. Mater. Chem. A 1 (2013) 9422–9426.

[188] B. Liu, Z. Zhang, K. Huang, Cellulose 20 (2013) 2081–2089.

[189] J.M.R. Gallo, R. Alamillo, J.A. Dumesic, J. Mol. Catal. A 422 (2016) 13–17.

[190] L. Geng, G. Yu, Y. Wang, Y. Zhu, Appl. Catal. A 427–428 (2012) 137–144.

[191] L. Geng, Y. Wang, G. Yu, Y. Zhu, Catal. Commun. 13 (2011) 26–30.

[192] X.Y. Liu, M.A. Huang, H. Ma, Z.Q. Zhang, J.M. Gao, Y.L. Zhu, X.J. Han, X.Y. Guo, Molecules 15 (2010) 7188–7196.

[193] D. Song, S. An, B. Lu, Y. Guo, J. Leng, Appl. Catal. B 179 (2015) 445–457.

[194] R. Liu, X. Wang, X. Zhao, P. Feng, Carbon 46 (2008) 1664–1669.

[195] X. Wang, R. Liu, M.M. Waje, Z. Chen, Y. Yan, K.N. Bozhilov, P. Feng, Chem. Mater. 19 (2007) 2395–2397.

[196] K. Malins, V. Kampars, J. Brinks, I. Neibolte, R. Murnieks, Appl. Catal. B 176–177 (2015) 553–558.

[197] Z. Gao, S. Tang, X. Cui, S. Tian, M. Zhang, Fuel 140 (2015) 669–676.

[198] D.R. Stellwagen, F. van der Klis, D.S. van Es, K.P. de Jong, J.H. Bitter, ChemSusChem 6 (2013) 1668–1672.

[199] Z. Sun, X. Zhang, H. Tong, Y. Liang, H. Li, J. Colloid Interface Sci. 337 (2009) 614–618.

[200] W.M. Van Rijin, D.E. De Vos, B.F. Sels, W.D. Bossaert, Chem. Commun. 34 (1998) 317–318.

[201] A.S. Dias, M. Pillinger, A.A. Valente, J. Catal. 229 (2005) 414–423.

[202] I. Muylaert, A. Verberckmoes, J. Spileers, A. Demuync, L. Peng, F. De Clippe, B. Sels, P. Van Der Voort, Mater. Chem. Phys. 138 (2013) 131–139.

[203] M. Hara, K. Nakajima, K. Kamata, Sci. Technol. Adv. Mater. 16 (2015) 34903–34924.

[204] A.J. Ragauskas, C.K. Williams, B.H. Davison, G. Britovsek, J. Cairney, C.A. Eckert, W.J. Frederick, J.P. Hallett, D.J. Leak, C.L. Liotta, J.R. Mielenz, R. Murphy, R. Templer, T. Tschaplinski, Science 311 (2006) 484–489.

[205] J.S. Luterbacher, D.M. Alonso, J.A. Dumesic, Green Chem. 16 (2014) 4816–4838.

[206] D.M. Alonso, J.Q. Bond, J.A. Dumesic, Green Chem. 12 (2010) 1493–1513.

[207] A. Corma, S. Iborra, A. Velty, Chem. Rev. 107 (2007) 2411–2502.

[208] M.J. Climent, A. Corma, S. Iborra, Green Chem. 16 (2014) 516–547.

[209] R. Rinaldi, F. Schut, ChemSusChem 2 (2009) 1096–1107.

[210] R. Rinaldi, F. Schut, Energy Environ. Sci. 2 (2009) 610–626.

[211] K. Wu, Y. Wu, Y. Chen, H. Chen, J. Wang, M. Yang, ChemSusChem 9 (2016) 1355–1385.

[212] M.J. Climent, A. Corma, S. Iborra, Green Chem. 13 (2011) 520–540.

[213] K. Wilson, A.F. Lee, Catal. Sci. Technol. 2 (2012) 884–897.

[214] J.M. Fraile, E. Garcia-Bordeje, E. Pires, L. Roldán, J. Catal. 324 (2015) 107–118.

[215] X. Mo, E. Lotero, C. Lu, Y. Liu, J.G. Goodwin, Catal. Lett. 123 (2008) 1–6.

[216] G. Chen, B. Fang, Bioresour. Technol. 102 (2011) 2635–2640.

[217] I. Ogino, Y. Suzuki, S.R. Mukai, ACS Catal. 5 (2015) 4951–4958.

[218] A.C. Alba-Rubio, F. Vila, D.M. Alonso, M. Ojeda, R. Mariscal, M. López Granados, Appl. Catal. B 95 (2010) 279–287.

[219] I. Sadaba, M. Lopez Granados, A. Riisager, E. Taarning, Green Chem. 17 (2015) 4133–4145.

[220] J.M. Anderson, R.L. Johnson, K. Schmidrohr, B.H. Shanks, Catal. Commun. 51 (2014) 33–36.

[221] X. Hu, C. Li, Green Chem. 13 (2011) 1676–1679.

[222] S. Van de Vyver, J. Geboers, P.A. Jacobs, B.F. Sels, ChemCatChem 3 (2011) 82–94.

[223] Y. Huang, Y. Fu, Green Chem. (2013) 1095–1111.

[224] J. Vanneste, T. Ennaert, A. Vanhulsel, B. Sels, ChemSusChem 10 (2017) 14–31.

[225] C. Zhang, H. Wang, F. Liu, L. Wang, H. He, Cellulose 20 (2013) 127–134.

[226] R. Ooms, M. Dusselier, J.A. Geboers, B. Op De Beeck, R. Verhaegen, E. Gobechiya,

J.A. Martens, A. Redl, B.F. Sels, *Green Chem.* 16 (2014) 695–707.

[227] Y. Jiang, X. Li, X. Wang, L. Meng, H. Wang, G. Peng, X. Wang, X. Mu, *Green Chem.* 14 (2012) 2162–2167.

[228] P.D. Cara, M. Pagliaro, A. Elmekawy, D.R. Brown, P. Verschuren, N.R. Shiju, G. Rothenberg, *Catal. Sci. Technol.* 3 (2013) 2057–2061.

[229] B. Liu, Z. Zhang, *ChemSusChem* 9 (2016) 2015–2036.

[230] G. Yang, E.A. Pidko, E.J.M. Hensen, *J. Catal.* 295 (2012) 122–132.

[231] J. Zhang, E. Weitz, *ACS Catal.* 2 (2012) 1211–1218.

[232] A.J. Crisci, M.H. Tucker, M. Lee, S.G. Jang, J.A. Dumesic, S.L. Scott, *ACS Catal.* 1 (2011) 719–728.

[233] S. Van de Vyver, J. Geboers, S. Helsen, F. Yu, J. Thomas, M. Smet, W. Dehaen, B.F. Sels, *Chem. Commun.* 48 (2012) 3497–3499.

[234] D.W. Rackemann, W.O. Doherty, *Biofuels Bioprod. Biorefin.* 5 (2011) 198–214.

[235] X. Qi, H. Guo, L. Li, R.L. Smith, *ChemSusChem* 5 (2012) 2215–2220.

[236] X. Guo, Q. Cao, Y. Jiang, J. Guan, X. Wang, X. Mu, *Carbohydr. Res.* 351 (2012) 35–41.

[237] J. Zhao, C. Zhou, C. He, Y. Dai, X. Jia, Y. Yang, *Catal. Today* 264 (2016) 123–130.

[238] R. Liu, J. Chen, X. Huang, L. Chen, L. Ma, X. Li, *Green Chem.* 15 (2013) 2895–290.

[239] B. Liu, Z. Zhang, *RSC Adv.* 3 (2013) 12313–12319.

[240] H. Wang, T. Deng, Y. Wang, X. Cui, Y. Qi, X. Mu, X. Hou, Y. Zhu, *Green Chem.* 15 (2013) 2379–2383.

[241] B. Karimi, H.M. Mirzaei, *RSC Adv.* 3 (2013) 20655–20661.

[242] K.I. Galkin, E.A. Krivodaeva, L.V. Romashov, S.S. Zaleskiy, V.V. Kachala, J.V. Burykina, V.P. Ananikov, *Angew. Chem.* 128 (2016) 8478–8482.

[243] R. Mariscal, P. Maireles-Torres, M. Ojeda, I. Sádaba, M. López Granados, *Energy Environ. Sci.* 9 (2016) 1144–1189.

[244] I. Agirrezzabal-Telleria, J. Requies, M.B. Güemez, P.L. Arias, *Appl. Catal. B* 145 (2014) 34–42.

[245] J. Iglesias, J.A. Melero, G. Morales, M. Paniagua, B. Hernández, *ChemCatChem* 8 (2016) 2089–2099.

[246] W. Liu, K. Tian, H. Jiang, H. Yu, *Sci. Rep.* 3 (2013) 2419–2425.

[247] I. Agirrezzabal-Telleria, J. Requies, M.B. Guemez, P.L. Arias, *Appl. Catal. B* 115–116 (2012) 169–178.

[248] T. Kim, R.S. Assary, C.L. Marshall, D.J. Gosztola, L.A. Curtiss, P.C. Stair, *ChemCatChem* 3 (2011) 1451–1458.

[249] S. An, D. Song, B. Lu, X. Yang, Y. Guo, *Chem. Eur. J.* 21 (2015) 10786–10798.

[250] D. Song, S. An, Y. Sun, P. Zhang, Y. Guo, D. Zhou, *ChemCatChem* 8 (2016) 2037–2048.

[251] B. Lu, S. An, D. Song, F. Su, X. Yang, Y. Guo, *Green Chem.* 17 (2015) 1767–1778.

[252] S. Zhu, C. Chen, Y. Xue, J. Wu, J. Wang, W. Fan, *ChemCatChem* 6 (2014) 3080–3083.

[253] A. Demolis, N. Essayem, F. Rataboul, A.C.S. Sustain, *Chem. Eng.* 2 (2014) 1338–1352.

[254] V.L. Budarin, J.H. Clark, J. Henschen, T.J. Farmer, D.J. Macquarrie, M. Mascal, G.K. Nagaraja, T.H.M. Petchey, *ChemSusChem* 8 (2015) 4172–4179.

[255] J.A. Melero, G. Morales, J. Iglesias, M. Paniagua, B. Hernandez, *Appl. Catal. A* 466 (2013) 116–122.

[256] F.D. Pileidis, M. Tabassum, S. Coutts, M. Titirici, *Chin. J. Catal.* 35 (2014) 929–936.

[257] D.A. Simonetti, J.A. Dumesic, *ChemSusChem* 1 (2008) 725–733.

[258] J.N. Chheda, J.A. Dumesic, *Catal. Today* 123 (2007) 59–70.

[259] T.M. Suzuki, T. Nakamura, E. Sudo, Y. Akimoto, K. Yano, *Microporous Mesoporous Mater.* 111 (2008) 350–358.

[260] T. Suzuki, T. Nakamura, E. Sudo, Y. Akimoto, K. Yano, *J. Catal.* 258 (2008) 265–272.

[261] S. Li, N. Li, G. Li, L. Li, A. Wang, Y. Cong, X. Wang, T. Zhang, *Green Chem.* 17 (2015) 3644–3652.

[262] G. Li, N. Li, J. Yang, A. Wang, X. Wang, Y. Cong, T. Zhang, *Bioresour. Technol.* 134 (2013) 66–72.

[263] M. Balakrishnan, E.R. Sacia, A.T. Bell, *ChemSusChem* 7 (2014) 1078–1085.

[264] R. Zhong, L. Peng, R.I. Iacobescu, Y. Pontikes, R. Shu, L. Ma, B.F. Sels, *ChemCatChem* 9 (2017) 65–69.

[265] R. Zhong, L. Peng, F. de Clippel, C. Gommes, B. Goderis, X. Ke, G. Van Tendeloo, P.A. Jacobs, B.F. Sels, *ChemCatChem* 7 (2015) 3047–3058.

[266] R. Zhong, F. Yu, W. Schuttyser, Y. Liao, F. de Clippel, L. Peng, B.F. Sels, *Appl. Catal. B* 206 (2017) 74–88.

[267] R. Zhong, Y. Liao, R. Shu, L. Ma, B.F. Sels, *Green Chem.* 20 (2018) 1345–1353.